NTNU

Norwegian University of
Science and Technology

BORON REMOVAL FROM MOLTEN SILICON BY GAS BLOWING USING DIFFERENT GAS MIXTURES

Claudio Sanna

Materials Technology
Submission date: July 2016
Supervisor: Gabriella Tranell, IMTE
Co-supervisor: Jafar Safarian, IMT

Norwegian University of Science and Technology
Department of Materials Science and Engineering

NTNU

Norwegian University of
Science and Technology

Master's Thesis
Spring 2016

Boron removal from molten silicon using different gas blowing mixtures

Author:
Claudio Sanna

Supervisors
Gabriella Tranell
Jafar Safarian

July 26, 2016

Preface

This Master's Thesis work was performed during spring and summer 2016 at NTNU laboratories at the Department of material science and engineering as the closing chapter of my two years studies in Innovative sustainable Energy Engineering.

Trondheim, 2016-07-26

Claudio Sanna

Acknowledgment

I would like to express my thanks firstly to my supervisor and co-supervisor, Gabriella Tranell and Jafar Safarian. Jafar has ever been present following me during the thesis and helping me with suggestions and especially with technical matters relative to the use of the laboratory, that often has been tricky. His patience was remarkable. Gabriella followed me all the year i spent at NTNU and gave me the opportunity to travel in Finland and US, her positivity and humanity are rare to find in professors.
I want to thank Akshay that helped me carrying out the experiments and has been the best companion i could ever expect in these two years of adventures across Denmark, Norway and the World.
Finally i want to thank my parents, that infected me with curiosity and broad-mindedness and supported me in every moment of this period, sharing my excitation and happiness for this experience.

(Claudio Sanna)

Contents

Chapter 1

Introduction

In this section the general overview of the present industrial situation in the field of silicon refining will be given. Moreover, it will encompass the objective of the research carried out.

1.1 Background

Starting from 2000 onwards, PV industry has increased exponentially and the global energy production from photovoltaic modules is estimated to be around 18GW in 2020.[1] Already in 2005, 90% of solar cells were made using crystalline silicon, back then 1.8GW of energy was derived from PV. This is the main reason why low-price refining and purification of metallurgical grade silicon (MG) to solar grade silicon (SoG-Si) is becoming ever more important.

To obtain SoG-Si, MG Silicon must be purified until 99,9999% (6N), which is a quite high purity standard, below the EG (electronic grade silicon) which is defined with 9N. There are 3 typical groups of impurities, defined like that:

1.Doping Elements (B,P)

2.Metallic (Fe,Ti,Al,Cu,Ca)

3.Light Elements (C,O,N)

Al for example is typically (1200-4000) ppm and Fe is (1600-3000) ppm [2]. While for these metallic elements we can allow up to a percentage of circa 10ppm in the solidified silicon melt, for the doping elements it is desired an extremely low percentage, $< 1ppm$.

This is due to the dopant effects these materials have on silicon, that diminish drastically the electronic properties of the silicon as a photovoltaic material. The traditional method for the production of SoG-Si is the Siemens process [3], a chemical route represented in Figure 1.1 in which the metallurgical silicon reacts with hydrochloric acid producing the gas trichlorosilane. The reaction is this one:

$$Si(s) + 3HCl(liq) \longrightarrow SiHCl_3(g) + H_2(g).$$

This gas has a higher purity than the metallurgical silicon, and it is then distilled and reduced to silicon in a CVD (chemical vapour deposition) reactor. The quantity of impurities obtained in the silicon are less than 0.02 ppm, but the cost of the process is very high. Solar industry needed more silicon and less purity compared to the semiconductor industry, for this reason the quest for new methods of silicon refining with lower costs became more important during time. The metallurgical route was proven to be more energy efficient and environmental friendly than the chemical route. Following a metallurgical route, metallic elements are typically refined with a directional solidification method, in which the melt is slowly solidified and impurities pushed away [4]. This method is called segregation. What happens is that when a silicon crystal grows, it is more energetically convenient to insert a silicon atom to the lattice then an impurity atom. This thermodynamic advantage leads to a lower concentration in the solid than

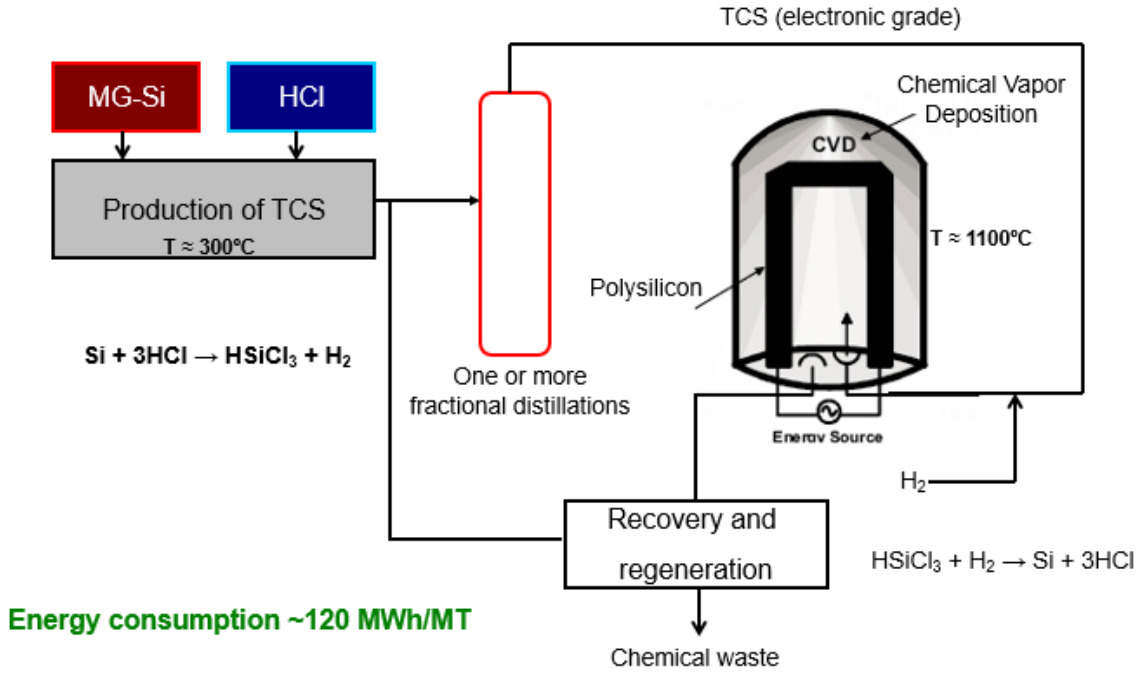

Figure 1.1: *Siemens Process* [3]

in the liquid due to a higher solubility of the impurity in the liquid [5]. At equilibrium the ratio between the two concentrations of components i is given by the coefficient K_i. Thus, when the solidification is slow enough and the K_i is very small, the impurities are mostly concentrated in the liquid part, making directional solidification an efficient method for impurities removal. This is typically possible when the segregation coefficient $K = \frac{C_{solid}}{C_{liquid}} << 1$, but while for example $K_{Fe} \sim 10^{-6}$ or $K_{Al} \sim 10^{-5}$, for the doping elements $K_B \sim 0.8$ and $K_P \sim 0.3$. With these high values, directional solidification doesn't work properly. Hence for these particular materials, this technique it is not adapt. Another method widely utilized for dispersed components, is the slag refining. A slag phase of $CaO - SiO_2$ is added to the silicon melt, these materials oxidize impurities and form a slag. The main point is that oxidized impurities have a higher solubility in the slag than in the silicon, thus they are removed with the slag. This process is very effective for impurities like Ca, Al, Mg and also effective for B as it will

be shown later in the literature survey, but not for P. Another method is the oxidative gas refining. O_2 is blown in the melt to oxidate the impurities in a slag, the result is shown in the graph depicted in Figure 1.2. It is noticeable how for example Ca and Al

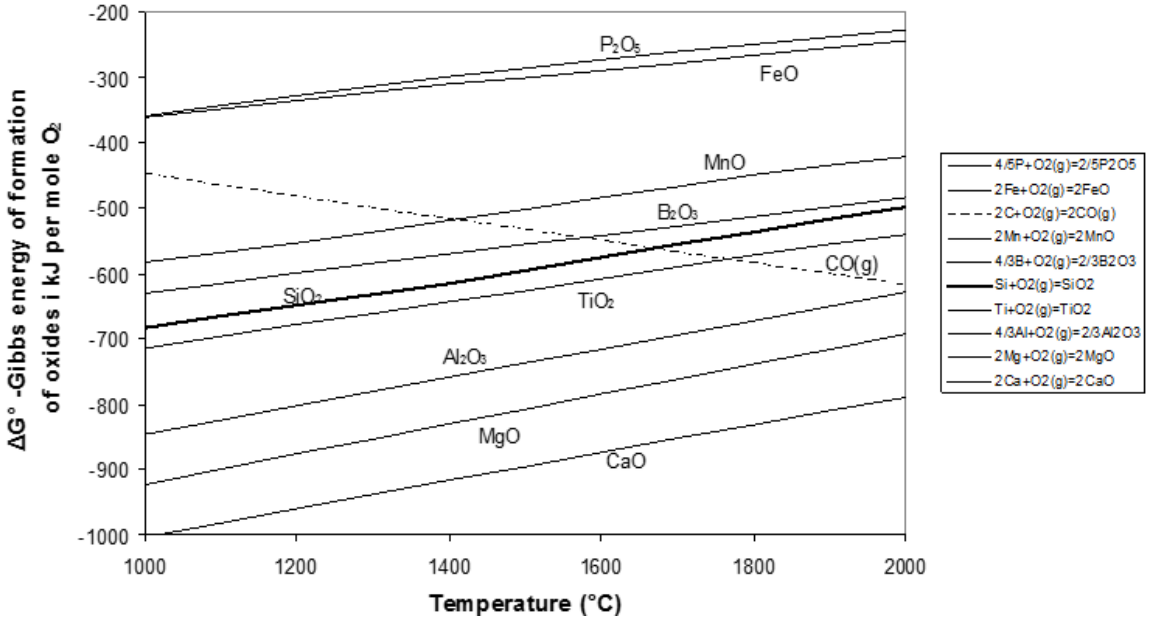

Figure 1.2: *Relative stability of elements/oxides [1]*

form more stable oxides than Si, and how B and P are less stable than SiO_2, with the consequence that their oxidation is in theory less easy. To refine P is currently used the vacuum refining technique, dissolved phosphorus has a volatility about 1000 higher than the one of silicon at 1823K, thus during evaporation the phosphorus content in the melt drastically decreases. Hence, considering these techniques, what still remains difficult to refine with a metallurgical route is Boron.

1.2 Objectives

Historically, Theurer in the 50's [6] was the first one to propose to blow a mixture of $H_2 - H_2O$ gas onto liquid silicon to reduce its boron content. The idea was to create

volatile products containing B that could be evacuated with the gas flow.

In the present Master's Thesis it is described the theory, experimental procedure and results behind 12 experiments performed at NTNU, regarding boron removal through gas blowing from 400g of molten silicon doped with 10ppm of B and 40ppm of P, using different gas mixtures. The doped solid silicon was put in a graphite crucible protected by carbon wool and mica roll and successively allocated inside an induction furnace that took the silicon above the melting point. Experiments were taken at circa 1 bar of pressure while the atmosphere was filled with Argon that flowed in and out the chamber, removing the volatile products created. The temperature was fixed 1823K for ten experiments and varied of +/- 50K for the remaining two. The other parameters that were fixed and the experimental setup will be discussed later in the work. Different combinations of gases with varying ratios were used:

Pure H_2, $H_2-2\%H_2O$, $H_2-4\%H_2O$, $H_2-6\%H_2O$, $50\%Ar-50\%H2$, $50\%Ar-50\%H_2-4\%H_2O$, $75\%Ar-25\%H_2-4\%H_2O$, $50\%He-50\%H_2$, $50\%He-50\%H_2-4\%H_2O$, $75\%He-25\%H_2-4\%H_2O$.

The purpose of the analysis was thus to confirm the result of precedent works made at NTNU with humidified hydrogen and have a better understanding of the role of the inert gases in the kinetics of the process of Boron refining. Finally it was desired to confirm the gas blowing technique in general as a promising method for boron removal from silicon and check whether P concentration varied in the experiments.

Various studies on metallurgical boron refining techniques, including gas blowing, will be described in the literature survey presented in the next pages.

Chapter 2

Theory

2.1 Literature Survey

In this section are presented the various metallurgical routes to Boron removal from silicon and discussed the most recent papers on gas blowing with $H_2 - H_2O$ mixtures.

2.1.1 Boron removal with slag refining

Slag refining was proposed as a metallurgical refining method relatively recently, in 1981 by Dietl and Wohlschlaeger [7]. Data for Boron removal with slag refining are so far still limited. Industrial production of SoG-Si through metallurgical routes was effectively carried out by Elkem Solar [8], using a combination of slag refining, acid leaching and directional solidification, Figure 2.1.

Figure 2.1: *Elkem Route [8]*

Here it will be discussed in particular the slag refining method, that was proven to

be particularly effective for boron removal. In order to do that were analyzed some works on the field, performed by Krystad et al. [10] and Jakobsson in his PhD [8]. The concept of slag refining is depicted in Figure 2.2, where (%x) is the concentration of metal in the slag phase and [%x] is the concentration of metal in the bulk phase.

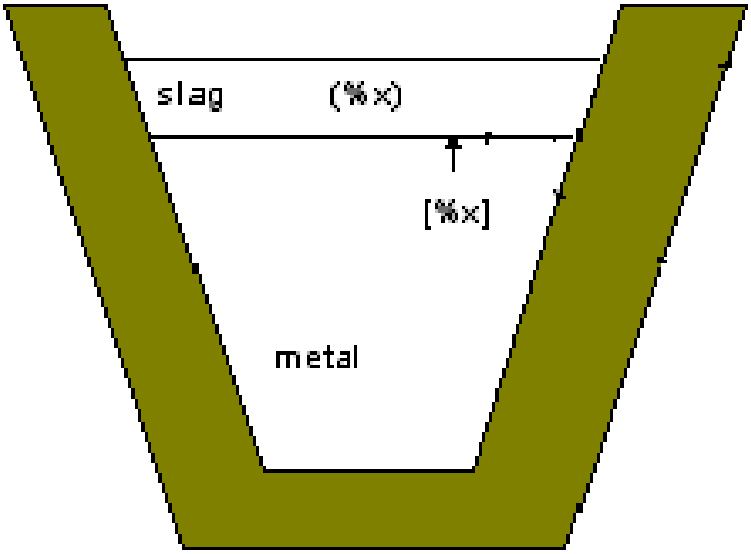

Figure 2.2: *Slag Refining [9]*

The slag, which is composed by oxides, is in chemical equilibrium with the metal phase that contains the impurities. The two liquids are immiscible. The reaction mechanism can be divided in this way:

First there is a mass transfer of the impurity from the bulk metallic phase to the boundary layer, then the impurity is diffused through the metal boundary layer. At the interface between metal and slag occurs the oxidation of the impurity, and lastly, from the slag boundary there is a transfer of the oxides to the slag bulk phase. Mass transfer is basically regulated by *natural convection* or *forced convection*. In the first case the driving forces are the temperature gradients and the density differences in the metal (viscosity,thermal conductivity) [9]. In the second case external forces are applied, like gas bubbling, mechanical stirring, pumping, or pouring to another ladle.

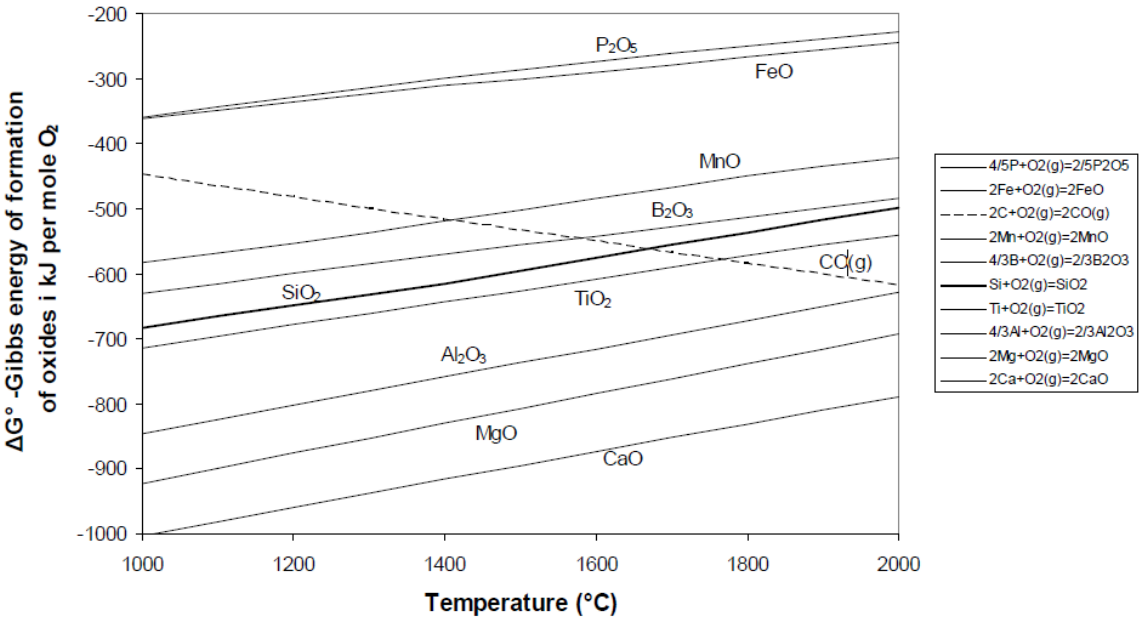

Figure 2.3: *Stability of Oxides [9]*

Crucial in order to obtain oxidation of the impurity, is that the stability of the oxide formed by the impurity is higher than the slag oxide. In case of the molten silicon [9], with SiO_2 as slag, oxides formed by the impurities will thus need to have a more negative Gibbs energy of formation, as resumed in Figure 2.3. All metal oxides less stable than SiO_2 will be reduced and will finish in the melt as contaminants. As can be seen, if we consider impurities like Ca, Mg or Al, they show higher stability and can readily be absorbed in the slag.

It is noticeable in the case of Boron, that B_2O_3 is a less stable oxide compared to SiO_2. It should create then a problem with slag refining, but this result, as shown in the thesis [8], is actually not valid in the case of molten silicon. Experiments showed that boron has a slightly higher affinity for the slag than expected, it has thus a positive deviation from ideal behaviour. It will be now described the process of boron slag refining from a chemical and thermodynamical point of view. The Chemical reaction happening at the interface is:

$$\underline{B} + \frac{3}{4}SiO_2 = \frac{3}{4}\underline{Si} + \frac{1}{2}BO_{1.5} \tag{2.1}$$

The thermodynamics is described by the equilibrium:

$$K = \frac{a_{B2O3}^{1/2} \times a_{Si}^{3/4}}{a_B \times a_{SiO2}^{3/4}} \tag{2.2}$$

where a_i are the activities of the elements described. The equation (4.4) shows how equilibrium will be moved to the right when boron has a positive deviation from ideal behaviour in molten silicon or negative deviation in slag.

In his PhD Thesis Jakobsson [8] used different slags, $CaO - SiO_2, MgO - SiO_2, CaO - MgO - SiO_2$ at 1873K and analyzed the distribution between silicon and the various slags.

Similar work was carried out by Krystad et al. 2012 [10], they used slag and silicon in a 1:1 or 1:2 ratio with a total mass of 30 grams at 1873K.

The reason for the importance of CaO and MgO as oxides in the slag, lies in their "basicity", in fact, they act as network breakers. Taking as example CaO, it dissociates in $Ca^{2+} and O^{2-}$ and boron reacts with the oxygen anions that come from the oxide, forming stabilized structures of Borate in the slag phase, BO_3^{2-}. The increased activity of SiO_2 and the increased concentration of oxygen anions can shift the equilibrium of B on the slag phase. Defining then the L_B ratio as $\frac{(\%B)}{[\%B]}$, where $(\%B)$ is the slag concentration of Boron, $[\%B]$ the bulk concentration of boron and the overall mass equation as:

$$\frac{[\%B] - [\%B]_\infty}{[\%B]_{in} - [\%B]_\infty} = exp(-\frac{k_t * \rho * A_s * t}{M} * (1 + \frac{M}{M_s * L_b})) \tag{2.3}$$

where $[\%B]_\infty$ is the boron concentration at the equilibrium, $[\%B]_{in}$ is the initial concentration, A_s the area of the slag metal, M the total mass of the metal, M_s the mass of the slag, ρ the total density, k_t the mass transport coefficient. Considering the

bulk-slag interface represented as Figure 2.4 where the driving force is the concentration

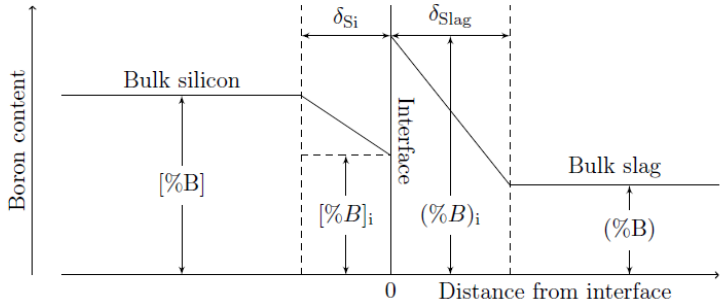

Figure 2.4: *Bulk-slag interface[8]*

gradient between the bulk silicon and the interface, it is possible from the last equation to obtain the B content in the metal as a function of time. Krystad et al. [10] found experimentally that the equilibrium time was approximatively two hours. The boron concentration with the use of different slags is summarized in Figure 2.5.

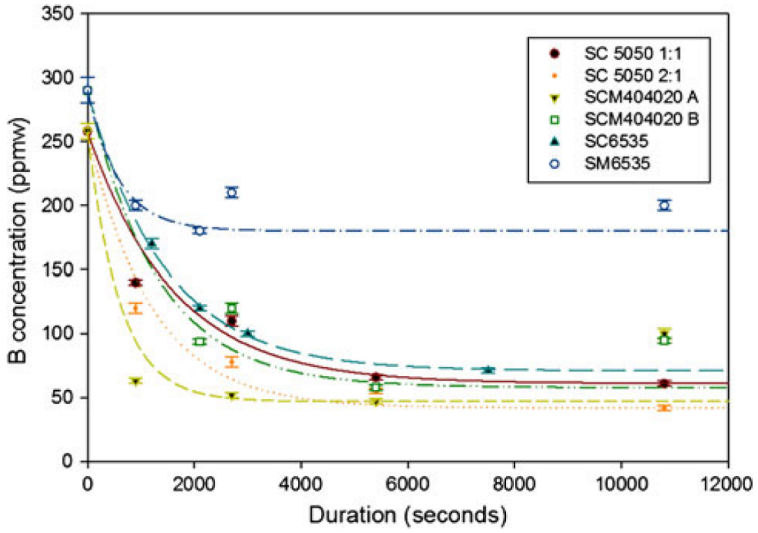

Figure 2.5: *Concentration of Boron [10]*

It can be seen that, given SC as silicon-calcium oxides, SM as silicon-Magnesium oxides and SCM as silicon-magnesium-calcium oxides, the graph shows how the best results in boron removal are obtained with the latter slag. Results from the PhD work

of Jakobsson [8] on the SCM (here CMS) slag are summarized in this table in Figure 2.6.

ID.	B in slag (ppmw)	B in Si (ppmw)	Mg in Si (ppmw)	Ca in Si (ppmw)
CMS1	65.1 ± 1.6	30.0 ± 4.3	293 ± 69	734 ± 125
CMS2	72.8 ± 6.0	33.9 ± 3.0	1354 ± 204	1726 ± 191
CMS3	83.1 ± 6.5	36.8 ± 2.9	2846 ± 383	3231 ± 436
CMS4	82.6 ± 5.6	37.7 ± 2.7	3862 ± 316	6264 ± 511
CMS5	69.6 ± 3.2	29.2 ± 2.8	1690 ± 321	13076 ± 1389
CMS6	90.3 ± 5.4	38.0 ± 5.2	1551 ± 216	265 ± 26
CMS7	78.7 ± 1.0	32.5 ± 2.7	3632 ± 328	8208 ± 986
CMS8	80.9 ± 6.6	33.6 ± 1.9	$2032 \pm 40^{\dagger}$	1710 ± 247
CMS9	71.1 ± 2.5	28.6 ± 1.4	975 ± 129	3139 ± 1059
CMS10	104.7 ± 9.3	42.3 ± 3.2	5113 ± 487	2010 ± 107
CMS11	99.9 ± 6.8	43.6 ± 1.0	3433 ± 420	656 ± 127
CMS12	110.6 ± 6.0	43.9 ± 3.9	2090 ± 234	155 ± 55
CMS13	102.3 ± 4.5	44.2 ± 1.4	5373 ± 326	5691 ± 703
CMS14*	37.3 ± 2.4	16.0 ± 0.9	7445 ± 794	6215 ± 826
CMS15	67.0 ± 1.8	29.4 ± 1.8	282 ± 29	346 ± 19
CMS16*	14.1 ± 2.1	7.7 ± 1.1	324 ± 42	342 ± 28
CMS17	75.1 ± 3.2	33.6 ± 0.8	$733 \pm 223^{\dagger}$	327 ± 96
CMS18*	23.4 ± 1.3	9.8 ± 1.0	775 ± 142	397 ± 69
CMS19	94.1 ± 10.4	38.3 ± 1.8	905 ± 51	92 ± 2
CMS20*	40.6 ± 1.8	16.1 ± 4.0	721 ± 166	$138 \pm 4^{\dagger}$

Figure 2.6: *Concentration of Boron [8]*

In the figure It is possible to see the trend of concentration of boron in 20 experiments with different percentages of oxides. The two works are both in accord with the conclusion that $CaO - MgO - SiO_2$ slag is the most effective in boron removal, and that can be used industrially as a boron refining technique. Krystad et al. [10] also show that Alumina slag should be avoided as can be seen in Figure 2.5. It has to be said on the other hand, that those results in the table show how solely slag refining is not sufficient to obtain satisfactory Boron levels to reach SoG-Si. Furthermore at ppm levels, uncertainty in B analysis are up to 30 % and L_B for the major part of the slags are in the area of 1-2. Additional refining steps are thus needed to bring the content to solar grade levels [8], i.e., Elkem processing.

2.1.2 Boron removal with $H_2 - H_2O$ gas mixtures

As it was quickly described in the introduction, the core of this technique proposed for the first time by Theurer [6], is to blow humidified hydrogen onto molten silicon. The reactions happening at the surface of the melt between the gas mixture and the molten $\underline{B}$ in the silicon create volatile species, for example HBO, BO or BH, that will thus reduce the content of B in the silicon. In Figure 2.7 it is depicted the blowing process and the different stages that lead to the production of volatile species containing B. The chemical reactions will be described in detail soon, after a short description of the technique. The silicon that contains the B impurities, is put inside a crucible with an extremely high melting point that is made of different materials. The crucible is placed in a furnace, in order to take the silicon above melting point and perform the removal. H_2 gas is humidified through a moisturizer with distilled H_2O and is blown onto the surface of the melt, where the chemical reactions start. The H_2O, has the striking role to provide oxygen for HBO formation, but also more hydrogen for the reactions. The atmosphere conditions in the chamber can vary according to the type of furnace or type of experiment. For example inside the chamber can be forced vacuum, or it can be filled with an inert gas, typically Ar or a mixture containing this gas. The inert gas typically flows in and out the chamber of the furnace, with the double role of avoiding oxidation of silicon and removing the volatile products formed. Oxidation of silicon in fact, it is a competitive reaction with respect to HBO formation and thus, as will be seen in the discussion of the next papers, is a factor that can reduce and limit the boron reactions at the interface. A detailed explanation of the process from a chemical and thermodynamical point of view will be now given.

In Figure 2.7 it is described a mass transfer system and the process of interaction between gases and molten boron is divided in stages. $\underline{B}$ is transported to the surface by convection and then diffuses in the boundary layer on the liquid side. The reactions

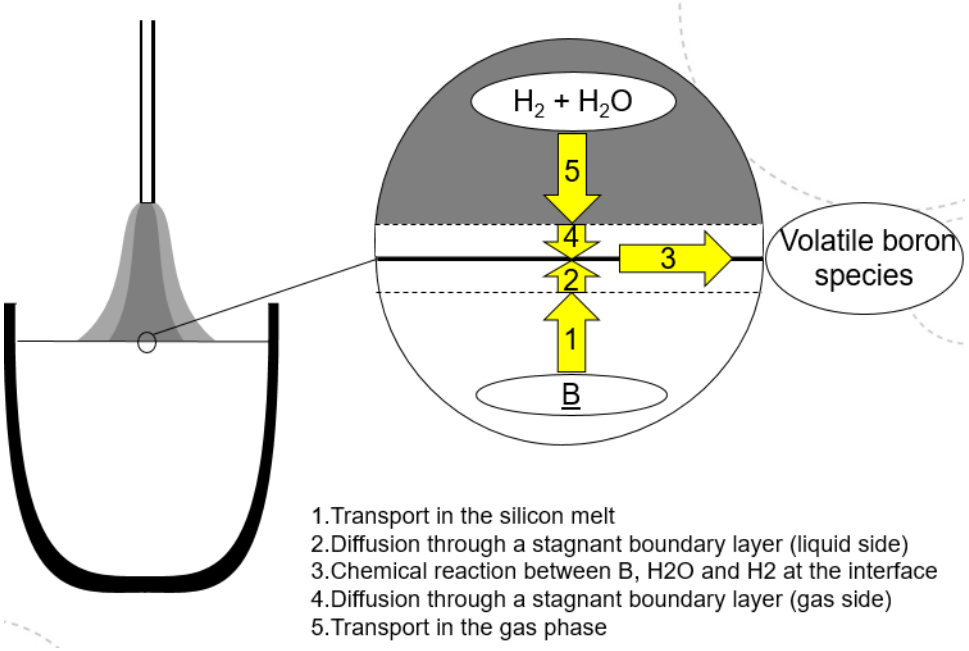

Figure 2.7: *Description of the process [11]*

happening at the gas-liquid boundary layer at a temperature above the melting point of silicon are these ones:

$$\underline{Si} + H_2O = SiO + H_2 \tag{2.4}$$

$$\underline{B} + H_2O = HBO + \frac{1}{2}H_2 \tag{2.5}$$

$$\underline{B} + SiO + \frac{1}{2}H_2 = HBO + \underline{Si} \tag{2.6}$$

The last equation (2.6) describes the equilibrium between dominant species. The rate of the reaction is:

$$r = k'' * [B]^l * [H_2O]^m * [H_2]^n \tag{2.7}$$

By integration of Equation (2.7) it is obtained the equation that was first discovered

by Theurer [6] and that describes the total process of boron removal from the system, hence the degree of B removal:

$$\ln(\frac{[B]}{[B]_0}) = -k * t \tag{2.8}$$

The constant k can be explained as the flow of the boron in the direction of the surface, it is important since it is a term of efficiency of the process [11]. According to the literature, the boron flux towards the silicon surface is independent of the mass of the silicon melt. Different studies [5] [11] [13] showed how boron removal rates increases with the oxygen or H_2O vapour concentration to the point that a layer of SiO_2 is formed. When the layer is formed on the surfaces the boron removal rate tends to decrease significantly. This, in the various experiments puts a limit on the concentration of oxygen content that can be used, higher concentrations tend to block the reaction of oxidation of the boron [12]. Hydrogen concentration plays an important role on boron removal rate as well. The study performed in the PhD thesis of J. Alteberend [5] showed that boron removal rate increases up to 50% of hydrogen concentration, after this boundary overcomes saturation. Suzuki et al.[5] attributed this effect to the thermal equilibrium between silica and Si(l) at the surface, which shifts towards Si(l) when hydrogen is added. They hypothesized that thermal conductivity of hydrogen could reduce as well the formation of the SiO_2 layer by increasing the temperature of the layer between the liquid and the gas phase. Silicon temperature increase has been shown from literature to decrease the rate of boron removal. This is a common result in the various papers analyzed that will be described in the next sections, where various results and conclusions coming from works on the field will be discussed.

Discussion on recent papers

In this section, results from the available papers on boron removal by gas blowing will be discussed and analyzed. It is interesting to observe how this technique evolved and was performed with different methods and gas mixtures.

The first paper to be analyzed will be the one of Khattak et al.[2], in which the B concentration present in a MG commercially available silicon was taken down to 0.3 ppm. The process was carried out in a HEM (Heat Exchanger Method) furnace followed by directional solidification. P was removed by vacuum processing as well as Al,Na,Mg. It was developed a thermodynamic model to analyze kinetic and equilibrium, the team used the software HSC.

In Figure 2.8 it is depicted the approach used to upgrade MG silicon to SoG-Si using HEM. The group states that experimentally the combination of the refining processes has shown better results compared to the sum of the individual processes. The HEM furnace had a cross-section of $69cm^2$ and it is depicted in Figure 2.9.

MG silicon was loaded in a fused silica crucible and placed in the HEM, initially the team used 1kg of MG, to reach up to 300 kg. The furnace was set up with an improved vacuum capability and ability to perform directional solidification.

The parameters varied in the experiment, were: gas composition, degree of vacuum, H_2 content of gas, water content of gas, temperature of molten silicon, lance diameter and height above the bath, flow rates. The melt was stabilized until 1723K, at this point the first sample was extracted. Various samples after different timings were extracted and analyzed with discharge mass spectroscopy and ICP emission spectroscopy. Sample extraction effected the melt, causing for example entrapment of gases, or inhomogeneities. A result to take into consideration was that the initially solidified ingot sample showed a lower level of impurities compared to the samples towards the last solidified material. Results of the process are shown in Figure 2.10.

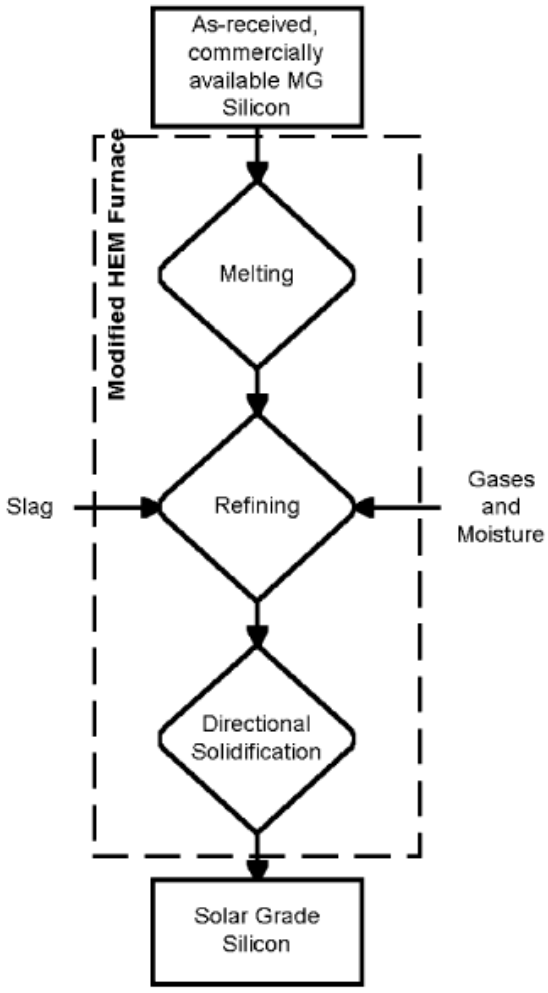

Figure 2.8: *Flow Diagram Process using HEM [2]*

1 Kg of MG silicon was refined using moist gas and the charge was directionally solidified after refining. Gas flow rates and moisture content were varied. 15 samples were extracted.

The lowest level is in M17, were the B content was measured to be 1.77 ppm. The team discovered that the process didn't lower the P concentration. M15 is thus the end of solidification and it is noticeable how B content increased. The team had now prove of the possibility of steady B reduction, and in the next part of the work tried to improve the efficiency of the reduction process. Models of dependence between rate constant

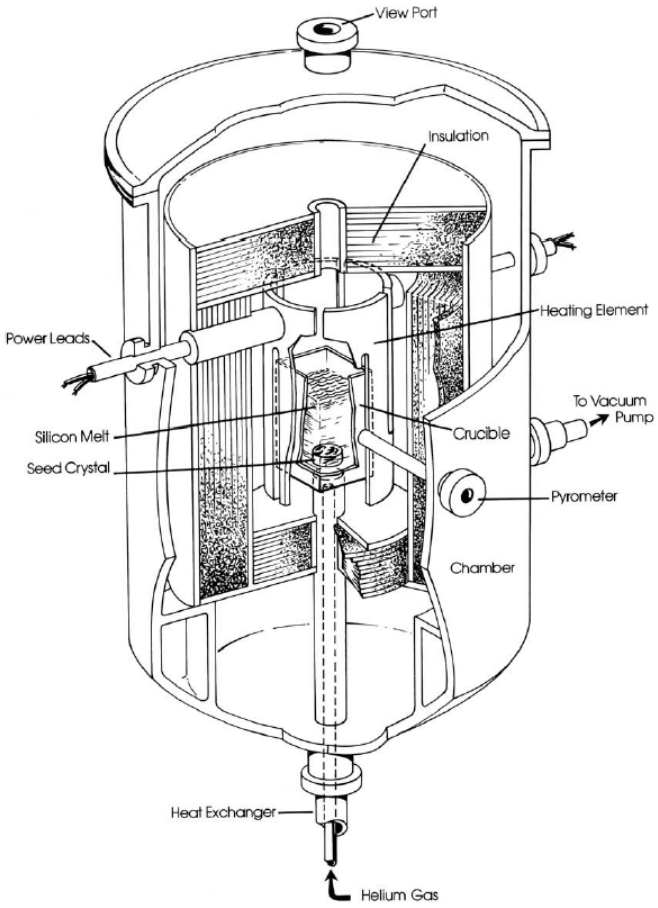

Figure 2.9: *HEM Furnace [2]*

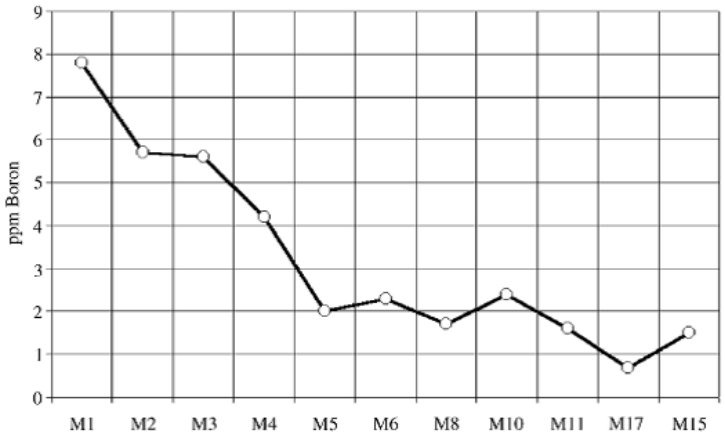

Figure 2.10: *Samples analyzed [2]*

and B concentration were used in order to estimate the refining time to bring B below 1 ppm. The directly proportional model appeared to be the most consistent with the

data. Half-life was reduced from 10h to less than 2h, and the final experiment with 50Kg of MG silicon showed that B could be reduced until 0.3 ppm.

The next paper analyzed in a chronological order is of 2008, performed by Morita et al.[1], a japanese team. Process and feasibility of boron removal with oxidizing refining were presented as results. It is quite interesting the thermodynamic equilibria analysis of molten silicon system in O_2 and $H_2O - O_2$ atmosphere that was shown together with setup and results.

The thermodynamic analysis aimed to find the limit of boron removal by calculating the Gibbs free energy and vapour pressure of gaseous species at different temperatures, to determine system pressure and gas composition. According to thermodynamic data, were considered different groups of oxidation, boron oxides of the family B_xO_y and hydrates BH_xO_y. For the intent of this survey, it will be neglected O_2 refining, but it is important to underline the results of the investigation. The thermodynamical analysis of the team for temperatures between 1600-2500K showed that B may be not oxidized in metallurgical grade silicon, because in this temperature region only Si oxidation takes place, with the formation of SiO_2 and SiO. Considering then the refining with $H_2O - O_2$ and thus the hydrates formed, with the thermodynamical tables NIST-JANAF the group listed the possible reactions happening at the surface, represented in Figure 2.11.

In Figure 2.12 relationship between ΔG^0 and temperature of the reaction is shown. It is clear from the picture how excluding HBO, the ΔG^0 of the reactions are all negative in the temperature range considered. Thus the preferential order of formation is $B_3H_3O_3 > HBO > BHO_2$ for increasing temperatures. The most easily formed are thus, at lower temperatures $B_3H_3O_3$, while at higher ones HBO and then BHO_2 .

If it is considered the partial pressure of the product $B_xH_zO_y$ vs temperature, from Figure 2.13 it can be seen that, the partial pressure of the $B_xH_zO_y$ hydrates excluding

Number	Reactions	Temperature range/K
(17)	$4[B]+2H_2O(g)+O_2=4BHO(g)$	1 685–6 000
(18)	$4/3[B]+2/3H_2O(g)+O_2=4/3BHO_2(g)$	1 685–6 000
(19)	$2[B]+2H_2O(g)+O_2=2BH_2O_2(g)$	1 685–6 000
(20)	$4/3[B]+2H_2O(g)+O_2=4/3BH_3O_3(g)$	1 685–6 000
(21)	$2[B]+2H_2O(g)+O_2=B_2H_4O_4(g)$	1 685–6 000
(22)	$4[B]+2H_2O(g)+O_2=4/3B_3H_3O_3(g)$	1 685–6 000
(23)	$4/3[B]+2/3H_2O(g)+O_2=4/9B_3H_3O_6(g)$	1 685–6 000

Figure 2.11: *Reactions creating hydrates [1]*

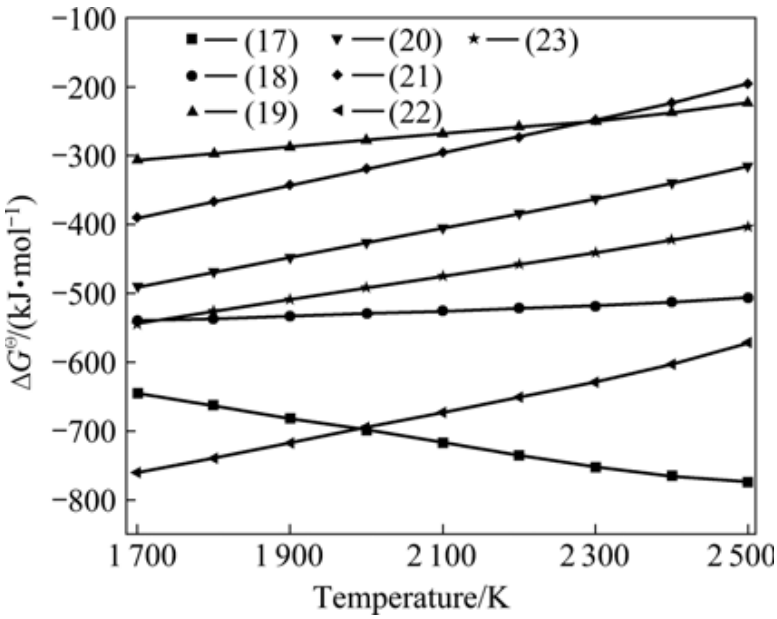

Figure 2.12: ΔG^0 *of chemical hydrates vs temperature [1]*

BHO is actually reduced at higher temperatures. This leads to the conclusion that in order to remove B more efficiently, the temperature above the melting point of silicon must be as low as possible, when this mixture of gases is used. From the thermodynamic equilibrium analysis of the team, appears clearly how with $H_2O - O_2$ gases, the refining rate is much higher than with O_2 gases, and that the temperature should be as low as possible above the melting point of silicon. The refining in this case was carried out in

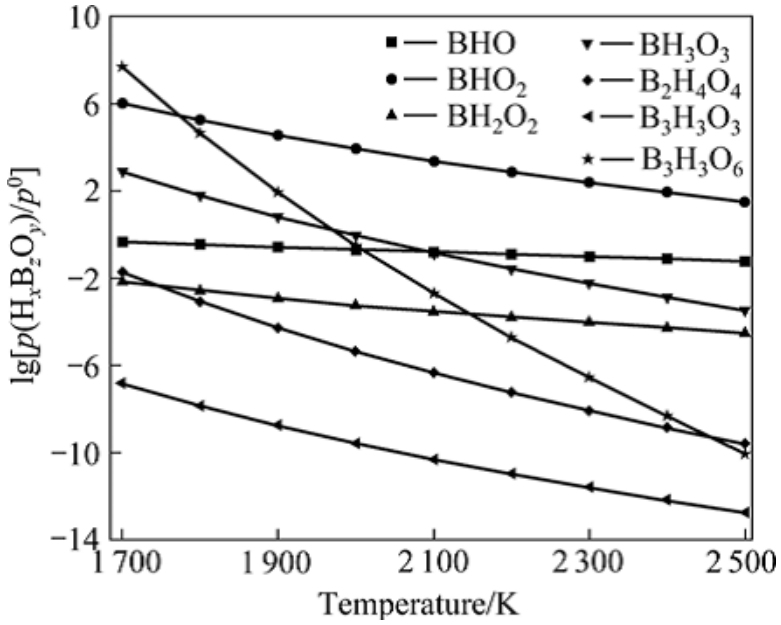

Figure 2.13: *Partial pressure of $B_xH_zO_y$ vs temperature [1]*

an electric arc furnace like the one in Figure 2.14 in which MG silicon 99.5% was refined in a $Ar - H_2O - O_2$ atmosphere at 10^{-4} Pa. The effect on the refining is similar to the one obtained in the work previously analyzed, as it can be seen in Figure 2.15. A big difference is the timing, after 10 minutes reduction of Boron is no longer happening.

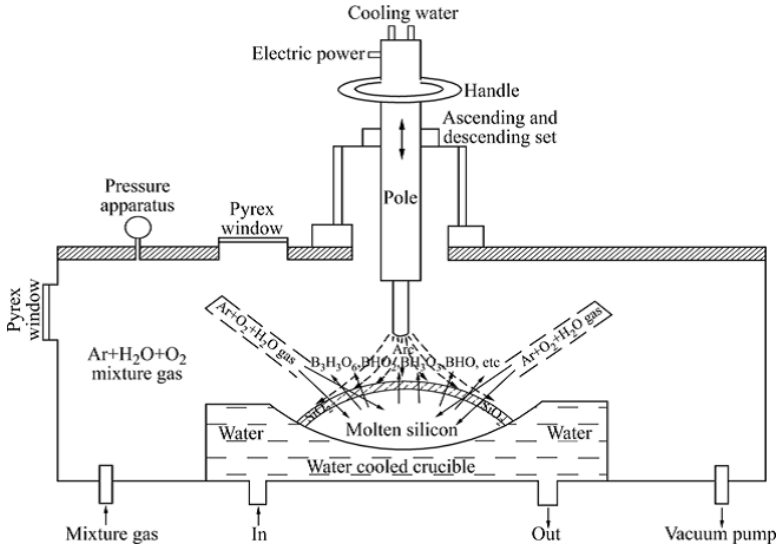

Figure 2.14: *Electric arc Furnace [1]*

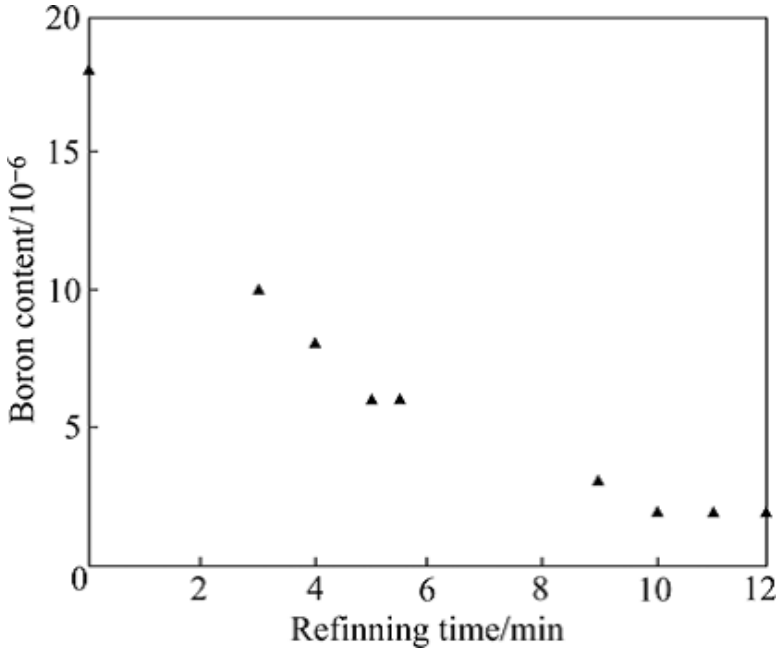

Figure 2.15: *Effect of refining on boron removal [1]*

The next paper that will be analyzed was made in 2012 by Nordstrand et al.[11] and uses a mixture of $H_2 - 3\%H_2O$ gases to refine boron.

Water-vapor-saturated hydrogen is used in this paper to remove boron doped in EG silicon in a vacuum frequency furnace. The team was able to reduce Boron from the initial value of 52 ppm to 0.7 ppm and 3.4 ppm at temperatures of 1723K and 1773K respectively. The experiment lasted 180 min. Exponential decay as in the other 2 works was observed and an interesting result is that after 99% of boron was removed, circa 90% of the silicon could be recovered.

Enthalpy and entropy of HBO formation were found with *Ab initio* calculations and a perturbative treatment of triple excitations [CCSD(T)] technique. In this way it was possible for the team to reproduce the experimental values within their uncertainties. The experimental setup consisted in EG B doped silicon (150 ppm) and a high-purity graphite crucible of the dimension of $70 \times 150mm$. For each measurement 210g of B-doped silicon was used. It was used a PtRh-Pt thermocouple that was put in contact

with the bottom of the crucible by a graphite tube, chamber was then closed to obtain vacuum. The system was then filled with hydrogen blown onto the melt with a quartz tube at a distance of 50mm. The hydrogen gas was saturated by water vapour and steam content fixed. Samplings were performed every 30 minutes through a quartz tube. Boron contents of the melt were measured using a resistivity meter. Hence, for each sample at least 8 points were measured with the meter. Results were then compared with ICP measurements. In Figure 2.16 it is shown the exponential decay in agreement with the other two works, while in Figure 2.17 it is interesting to see how resistivity measures closely agree with ICP analysis. As an important result, in complete agreement with the precedent work, it is shown that 99% of boron removal happens at 1723K, while only 93% happens at 1773K. Hence, a lower temperature favours boron removal. The conclusion of the team was that as the rate of boron removal increases with decreasing temperature, it indicates that the process is controlled by chemical reactions occurring in the gas-liquid interface.

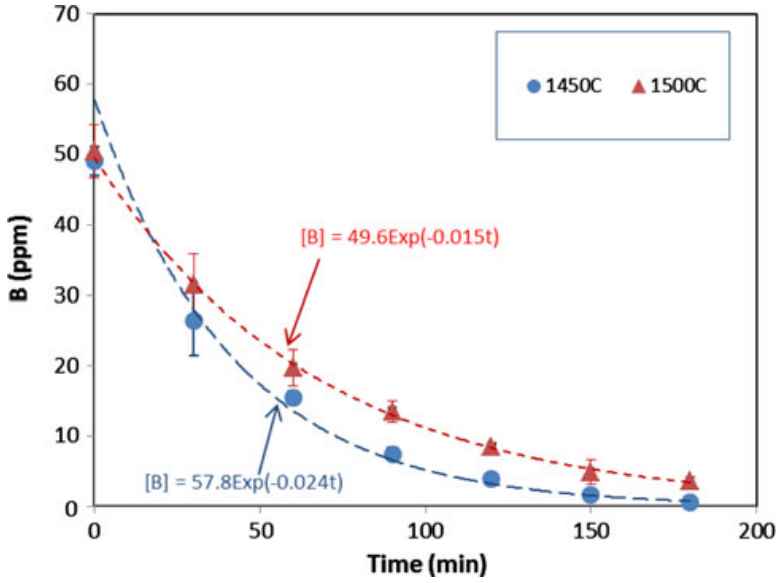

Figure 2.16: *Boron Removal [11]*

The following paper written by J.Safarian et al.[12] analyzes the Boron removal

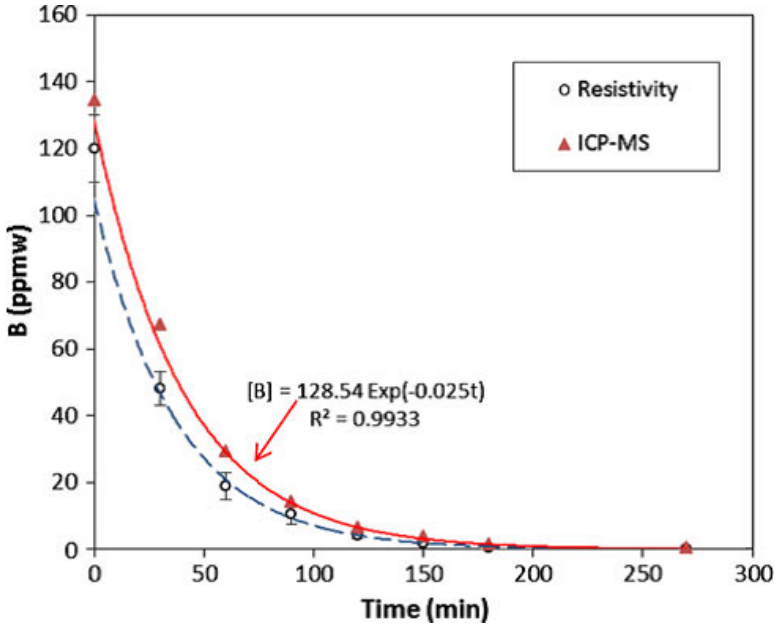

Figure 2.17: *ICP vs Resistivity measurements [11]*

from molten silicon with a different mix of gases, humidified Ar, N_2, H_2. Kinetics and removal of B are investigated for every type of gas, and thermodynamics is studied to explain experimental observations.

The experimental setup is the one in Figure 2.18. EG silicon (9N) was B-doped and melted in a graphite crucible inside an induction furnace in an Argon atmosphere.

The experiment lasted 60 minutes and the temperature of the melt was kept at 1873K. The temperature was measured by a thermocouple type C located in an alumina insulating tube.

The different gases at (5N), humidified, were blown over a 400g B-doped Si-melt and the partial pressure of oxygen continuously measured. A Window on top allowed the team to insert a quartz sampling tube and observe the formation of condensed phases over the melt. Again resistivity measures were taken and compared with ICP analysis. Details of the experiment are depicted in Figure 2.19.

During the experiments was found that an oxide surface layer was formed over

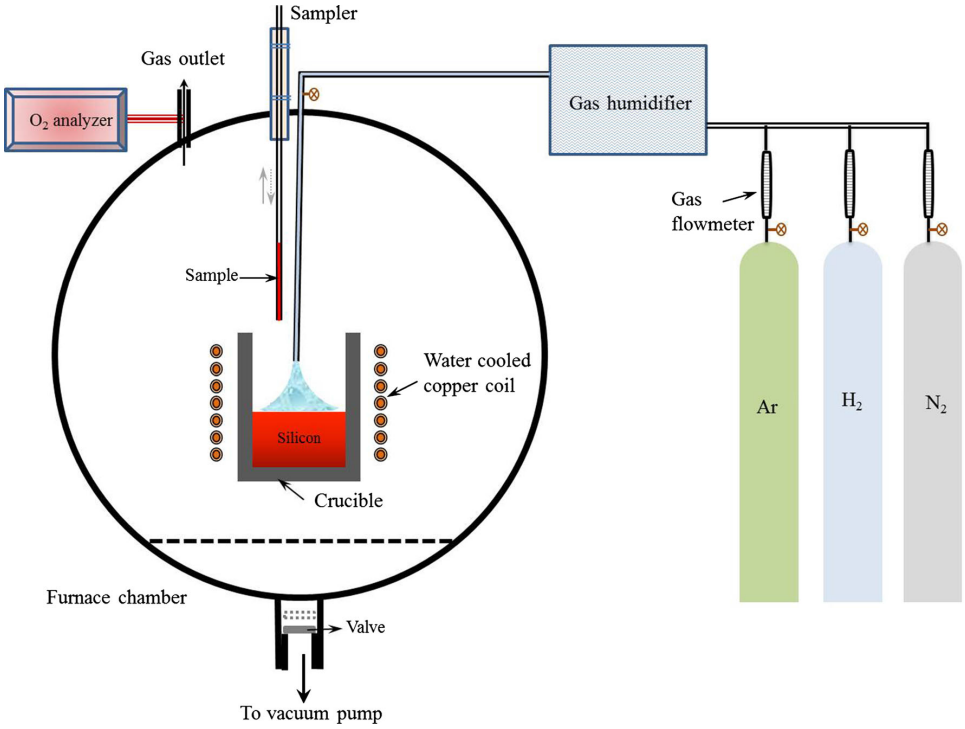

Figure 2.18: *Experimental setup [12]*

Exp. Number	Gas Composition (Vol Pct)	Refining Temperature [K (°C)]	Concentration of B ($C_{B,t}$) at Refining Time t Measured by ICP-MS (ppmw)					$C_{B,t}$ (ppmw), Resistivity Measurement
1	Ar-3 pctH_2O	1703 (1430)	$C_{B,0}$ = 24.8	$C_{B,25}$ = 19.1	$C_{B,60}$ = 16.81	$C_{B,180}$ = 15.9		$C_{B,180}$ = 18.5
2	N_2-3 pctH_2O	1703 (1430)	$C_{B,0}$ = 24.8	$C_{B,25}$ = 20.42	$C_{B,60}$ = 19.6	—		$C_{B,60}$ = 19.7
3	H_2-3 pctH_2O	1703 (1430)	$C_{B,0}$ = 24.8	$C_{B,5}$ = 21.9	$C_{B,25}$ = 15.8	$C_{B,60}$ = 9.8	$C_{B,180}$ = 2.01	$C_{B,180}$ = 2.1
4	H_2-5.9 pctH_2O	1773 (1500)	$C_{B,0}$ = 28.3	$C_{B,5}$ = 24.7	$C_{B,15}$ = 20.9	$C_{B,30}$ = 17.5	$C_{B,60}$ = 14.5	$C_{B,60}$ = 16.96
5	H_2-11 pctH_2O	1773 (1500)	$C_{B,0}$ = 28.6	$C_{B,5}$ = 24.7	$C_{B,15}$ = 22.2	$C_{B,30}$ = 16.5	$C_{B,60}$ = 12.6	$C_{B,60}$ = 10.8
6	H_2-3 pctH_2O	1803 (1530)	$C_{B,0}$ = 12.4	$C_{B,5}$ = 12.1	$C_{B,30}$ = 9.01	$C_{B,60}$ = 6.85		$C_{B,60}$ = 6.4

Figure 2.19: *Details of the experiment and B concentrations in treated silicon melts [12]*

the silicon during refining, this surface was then analyzed by EPBMA (electron probe microanalysis) technique. One of the most interesting results of the paper is that the lower equilibrium partial pressure of HBO gas at higher temperatures causes a slower B removal rate. Furthermore it was proposed a mechanism for HBO formation.

It is initially reported the Gibbs energy for $HBO(g)$:

$$B + \frac{1}{2}H_2 + \frac{1}{2}O_2 = HBO(g) \tag{2.9}$$

$$\Delta G^0 = -229.4 - 0.2029T(kj/mol) \tag{2.10}$$

The proposed equation for HBO formation is:

$$\underline{B} + SiO + \frac{1}{2}H_2 = HBO + \underline{Si} \tag{2.11}$$

The team explains that SiO gas in this reaction is produced through simultaneous oxidation of silicon with H_2O. Refining method and reactive gas composition determine the kinetics of B removal. An important result observed by the team was that the oxygen partial pressure is rapidly decreasing in the furnace during heating, and the explanation proposed is that the decrease is due to the fast interaction of oxygen with the graphite crucible with increasing temperature and CO gas formation. It was observed a short rise in p_{O2} at the start of the melting with a subsequent decrease during the refining step with the introduction of humidified gases. This effect, shows that the free oxygen in the gas phase during refining is at a low level. The group found out that ICP measures were in good agreement with the resistivity measures and to evaluate the degree of B removal, it was used the following equation:

$$F_B = 100 * (1 - C_{B,t}/C_{B,0}) \tag{2.12}$$

where $C_{B,0}$ is the initial B concentration and $C_{B,t}$, B concentration at refining time t. For the given time, 60 minutes, it was found that for all the experiments, the B removal with H_2 humidified gas is higher than for Ar and N_2 gases. For longer refining times, the team found out that gases show different behaviours and B removal kinetics is different. Effect of temperature of the molten silicon was found to be consistent with the previous works. The SiO_2 layer was analyzed, it showed to be porous to a X-ray analysis and showed up in most of the experiments after 30 minutes. Relationship between refining time and B concentration was described as:

$$\ln(\frac{C_{B,0}}{C_{B,t}}) = k_B * (A/V) * t \tag{2.13}$$

where A/V is the ratio of the melt surface on the melt volume, while k_B is the total mass transfer coefficient for B removal from the melt to the gas phase. It was observed that the slower B removal for other experiments after some refining time was due to the formation of the oxide layer, that decreases the effective A/V ratio. The equation that describe its formation is:

$$Si + H_2O(g) = SiO_2(s) + H_2 \tag{2.14}$$

It is interesting to see that for experiments 4 and 5 in Figure 2.19 the layer was observed after 30 minutes while in experiment 6 no oxide layer was observed. The researchers propose as explanation that for a given H_2O content in the gas, the passive layer is less stable at higher temperatures, in fact experiment 6 is held at higher temperatures compared to others. It was found that B removal rate increased with increasing of H_2O content in the refining phase as long as the oxide layer is not covering the surface. The experiments showed agreement with the previous works regarding the fact the B removal is decreased with increasing temperatures. A representation of the results of the various experiments is shown in Figure 2.20.

Furthermore the team confirms the results of the previous studies that hydrogen plays a key role in the reaction mechanism since B removal rate is faster with H_2 than with the other gases. The team proposes to explain this effect considering that hydrogen is dissolved in silicon and that B removal occurs through the interaction of the dissolved B and H species with H_2O gas at the melt-gas interfacial area. if we consider in fact this reaction:

$$\underline{B} + \underline{H} + H_2O = HBO(g) + H_2 \tag{2.15}$$

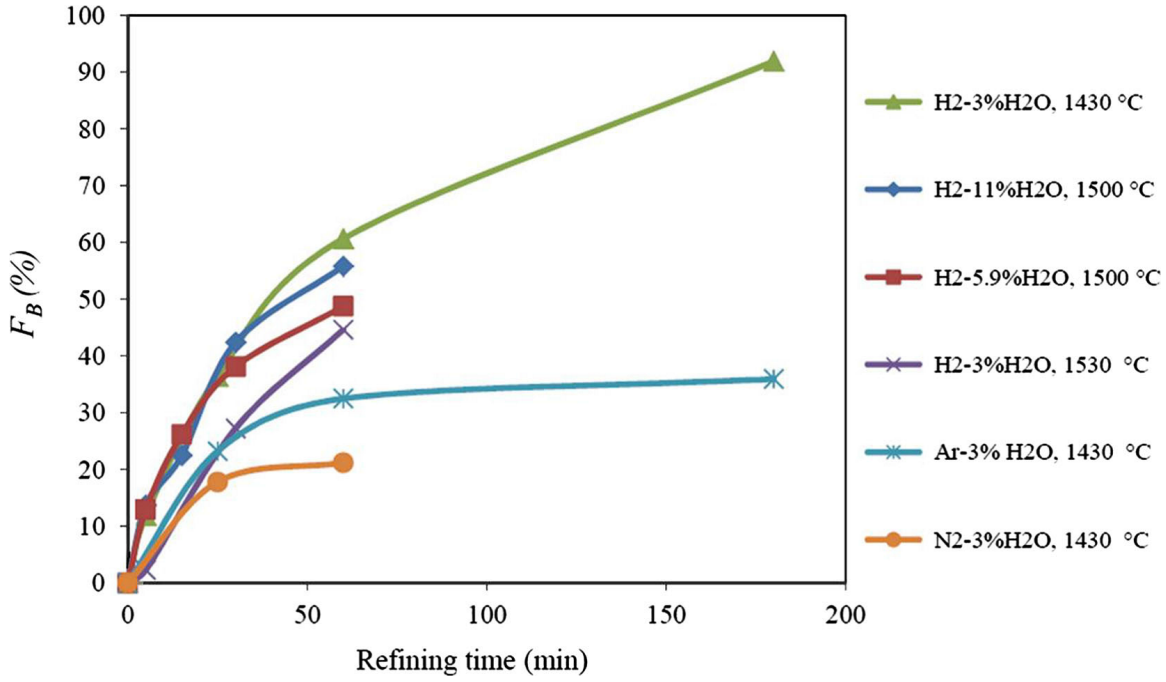

Figure 2.20: *Boron removal degree in silicon refining by humidified gases [12]*

The process requires a considerable amount of hydrogen to provide enough dissolved atomic hydrogen close to the reaction interface. It is suggested that this may explain the faster B removal with increasing the H_2/Ar ratio in $Ar - H_2 - H_2O$. Another observation was that the dissolved oxygen is not considered as a major contributor in the B removal reaction mechanism, and they report that other researchers suggested that the presence of H_2 suppresses the formation of SiO_2 by oxidation of SiO in the gas boundary layer, hence enhancing the diffusion rate of HBO products. In addition to that it is interesting to show the obtained results for the melt treatment at different temperatures showed in Figure 2.21. It is shown that among the B-containing species the partial pressure of HBO(g) is the highest in the system and HBO is the most easily formed hydrate. An other result that the group tried to explain, is that the thermodynamic calculation showed the existence of solid SiO_2 in the system coexisting with a significant amount of SiO gas. The explanation proposed is that the reason of not observing a passive oxide layer for some experiments is due to the lack of solid

SiO_2 nucleation on the silicon surface. Explanation supported by the fact that the oxide layers have been observed at least after 30 minutes from the start of the refining. Higher stability of SiO gas at higher temperatures may actually reduce the possibility of the layer formation, situation clearly seen in experiments 3 and 6. Figure 2.21 lastly shows that the equilibrium partial pressure of the HBO gas is decreased with increasing temperature. Thermodinamically speaking, that means a smaller driving force for the reaction (2.15) at the melt surface and therefore a lower B removal rate.

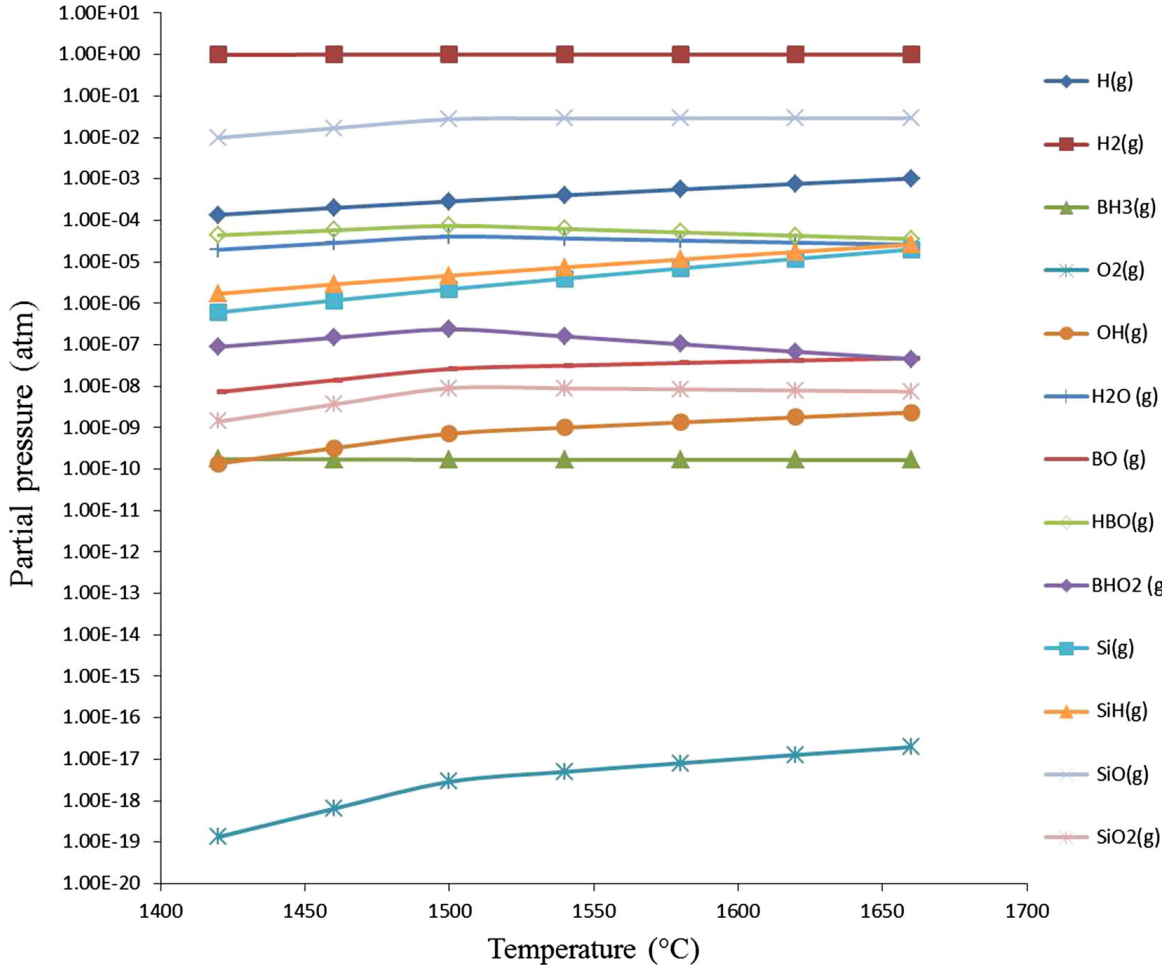

Figure 2.21: *Equilibrium partial pressures of gas components above a 400g silicon melt containing 30ppm B under H2-3 pct H2O atmosphere [12]*

The most recent paper, that will be described now, was written again by a NTNU team guided by J. Safarian and G.Tranell [19], and analyses mechanisms and kinetics

of Boron removal with humidified gases in a thorough paper, in which gas blowing over silicon melt has been performed varying different variables in order to understand which mechanisms and experimental conditions influence the rate of boron refining.

The group used an experimental setup like the one in Figure 2.18. Results confirmed the decrease in Boron removal with increasing temperature, and this is said to be due to the competitive reactions between silicon and oxygen as well as boron and oxygen. Furthermore they showed how an increase in gas flow rate over the melt increases refining thanks to a better supply and transport of the gas over the melt surface. This was confirmed by CFD modeling. The group also proposes that the rate of B removal is controlled by the rate of dissolved oxygen supply to the system, in addition to the mass transport in the gas phase.

They observed how $H_2 - H_2O$ mixes of gas performed better compared to other kind of humidified mixes, for example Argon and Nitrogen. Other interesting results were obtained changing type of crucibles for the refining process, and it was discovered how Al_2O_3 tended to perform better since it provides additional boron gasification with products like $AlBO_2$. $AlBO_2$ properties were hence revised with quantum chemistry calculations.

The group performed various types of experiments varying different parameters. The list of the experiments with results is listed in the next Figure 2.22. It can be seen how the following parameters were changed: Crucible type, Temperature, Lance diameter, Lance distance to melt surface, Gas Flow rate.

When lance diameter and gas flow rate were changed, the observation of the results showed that rate of B removal significantly increased with increasing flow rate and that led to the conclusion that gas flow rate is more important than velocity of gas for the kinetics of B removal. This is shown in Figure 2.23 and 2.24 .

It is clear how experiments with 9L/min led to the best refining. When the Lance

Exp. No.	Crucible Type	Temperature [K (°C)]	Lance Diameter (mm)	Lance Distance to Melt Surface (mm)	Gas Flow Rate (NL/min)	Mass Transfer Coefficient (m/s)
1	graphite	1703 (1430)	4	30	0.5	2.0×10^{-6}
2	graphite	1703 (1430)	4	30	1.5	3.3×10^{-6}
3	graphite	1703 (1430)	4	30	3	1.3×10^{-5}
4	graphite	1703 (1430)	2	30	0.5	1.5×10^{-6}
5	graphite	1703 (1430)	2	30	1.5	5.1×10^{-6}
6	graphite	1703 (1430)	2	30	3	9.4×10^{-6}
7	graphite	1703 (1430)	2	30	6	1.9×10^{-5}
8	graphite	1703 (1430)	2	30	9	2.5×10^{-5}
9	graphite	1703 (1430)	2	10	6	1.3×10^{-5}
10	graphite	1703 (1430)	2	50	6	1.7×10^{-5}
11	graphite	1803 (1530)	4	30	3	7.0×10^{-6}
12	graphite	1803 (1530)	2	30	6	1.3×10^{-5}
13	alumina	1773 (1500)	2	30	3	2.1×10^{-5}
14	quartz	1703 (1430)	2	30	3	1.5×10^{-5}
15	quartz	1773 (1500)	2	30	3	1.4×10^{-5}

Figure 2.22: *List of Experiments performed by NTNU Group [19]*

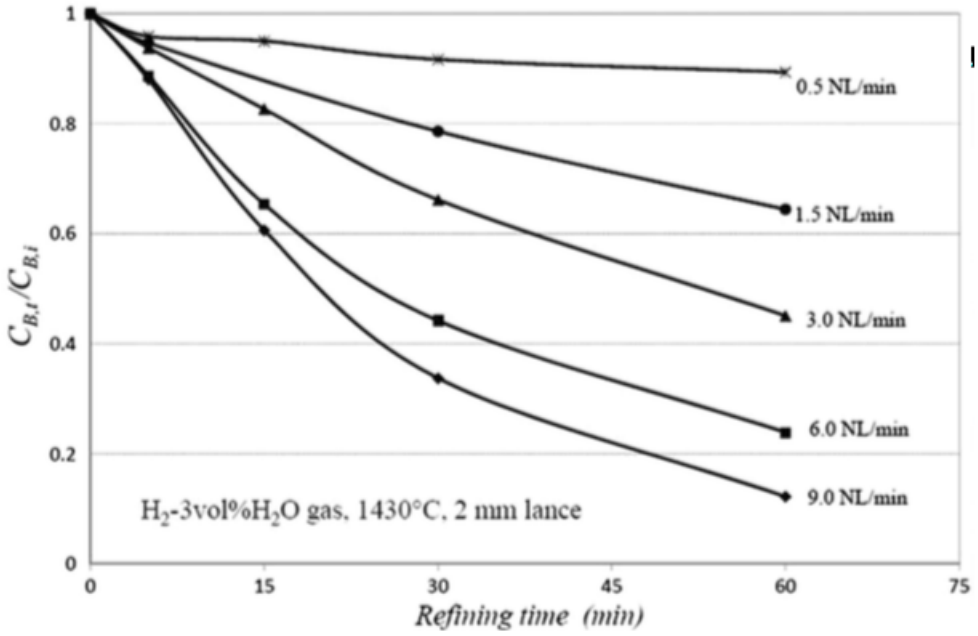

Figure 2.23: *Experiments with variation of Gas flow rate [19]*

distance was the closest to the melt they obtained the lowest values of Boron removal. Change in temperature produced effects already expected, its increase reduce the performances of the process.

When the crucible was changed, Alumina gave the better refining rates, the quartz performed better than the graphite. A description of the mechanisms of B removal

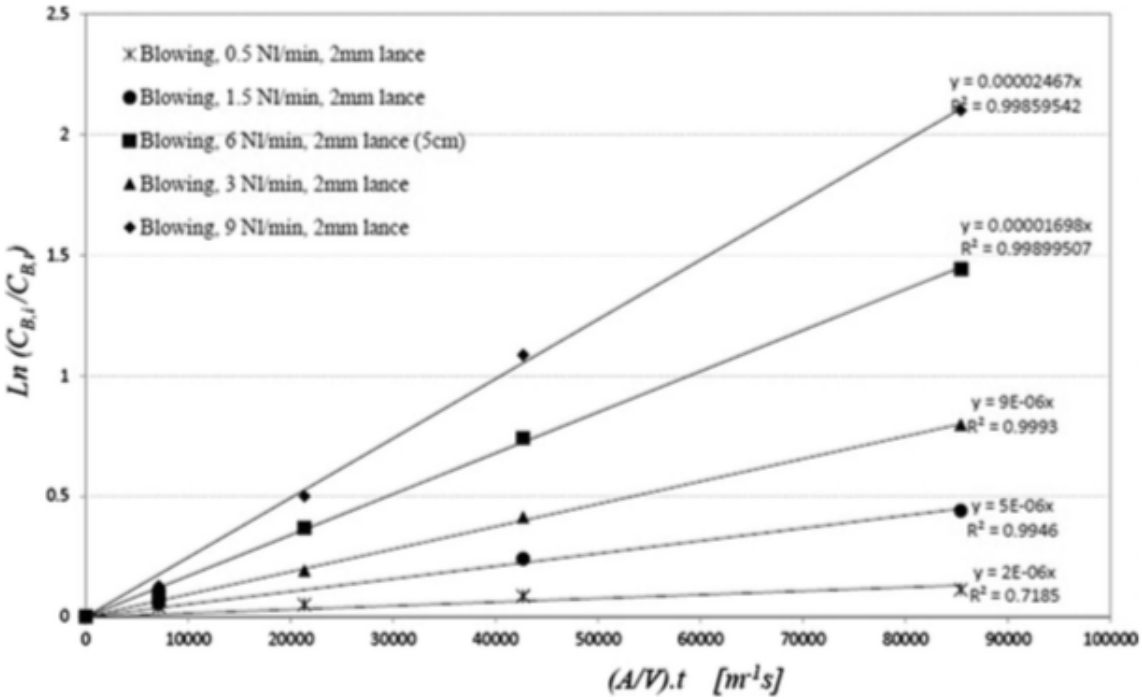

Figure 2.24: *Experiments with variation of Gas flow rate, different graph [19]*

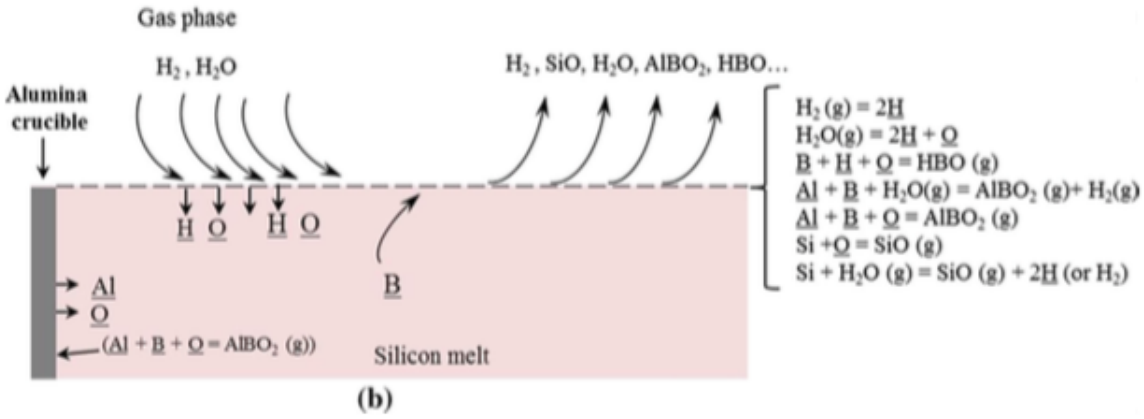

Figure 2.25: *Mechanisms of B removal in Al2O3 crucible [19]*

and Si loss for alumina crucible, that helps to understand the reactions involved in the process can be observed in Figure 2.25. The faster B removal in a quartz crucible is attributed by the group to a higher activity of the dissolved oxygen, while for alumina

as already said, the faster removal is attributed to the the Al_2O_3 reactions that adds up to reaction (2.15). Another interesting part of their work is relative to SiO formation. The group states that its formation is driven by this formula:

$$Si + \underline{O} = SiO(g) \tag{2.16}$$

SiO produced in this way affects HBO formation. The ratio between their partial pressured showed also how formation of SiO is more favoured than HBO since SiO activity is higher. When temperatures are kept lower, activity of SiO reduces, favouring HBO formation, thus rate of dissolved oxygen supply is important.

2.1.3 Plasma Refining

Another technique for boron refining which is important to mention is plasma refining. Various papers were analyzed on this topic. The principle of plasma refining consists in the use of plasma gas containing oxidation species which is drawn on the surface of liquid silicon [15]. This leads to the reaction of the impurities inside the molten silicon with the reactive gases.

The result is the creation of volatile species. As described in previous works [16], boron with addition of oxygen and hydrogen will evaporate mainly in the form of HBO and BO. As shown in the study of Nakamura [17] a higher molten silicon temperature causes preferential boron oxidation thus increasing the reaction surface temperature by plasma heating this is more effective. The experimental setup is depicted in Figure 2.26. The apparatus consists in an inductive plasma torch that is combined with an inductive cold crucible. Fusion of the silicon is initiated by the plasma torch. When the volume of the liquid phase at the top of the crucible increases enough, then the induction power takes over. The process takes place in an atmosphere-controlled, water

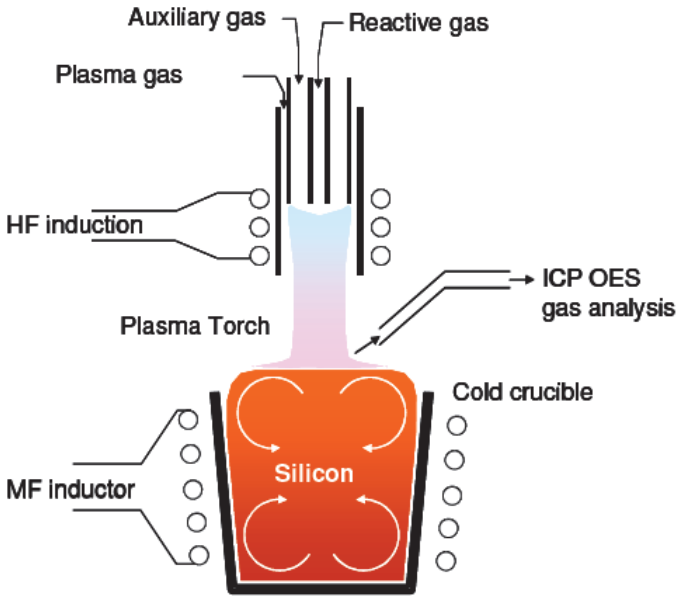

Figure 2.26: *Experimental setup [15]*

cooled chamber. The plasma torch is made of three concentric tubes, and an injector is used to inject reactive gases mixed with argon into the plasma [15]. It is interesting to point out that plasma power is 30 kW while induction frequency is 3.4 MHz, at these conditions the cold crucible does not allow direct fusion of the silicon. Pressure is stabilized by means of a valve. The gases are then sampled in a chamber through ICP analysis. The main reaction happening on the surface is:

$$\underline{B} + H_2O(g) = BO(g) + H_2(g) \tag{2.17}$$

while happens also an oxidation of Silicon in SiO species and HBO formation.
The whole process, as described by Fourmond et al.[15] happens in various steps. Once the volume of the liquid phase at the top of the crucible is sufficient and induction power takes over, silicon powder is injected in the bath by means of the axial tube of the plasma torch. The purification process starts when the entire solid silicon is melted. At this point oxygen and hydrogen are injected on the surface through the axial tube and reactions begin. Results of the group guided by Fourmond [15] are depicted in

terms of B/Si in Figure 2.27 where temperature difference of 150 °C between two

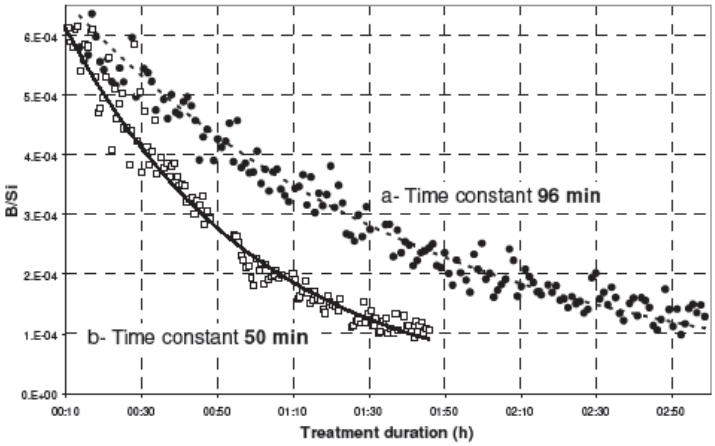

Figure 2.27: *Results [15]*

cases was adjusted by means of the power applied to the cold crucible. The boron, as found also in the previous papers, also in this case decreases exponentially with a time constant that in these two experiments varies with the temperature. In one case is 96 minutes, in the other, with a higher temperature, of 50 minutes. This indicates that boron volatilization increases with higher silicon temperature. The team observed, in accord with the experiments of gas blowing removal, that the formation of silica layer on the surface is a limiting phenomenon in the volatilization process. The team of Nakamura et al.[17], performing a similar experiment with steam-added plasma melting method represented in Figure 2.28 investigated on the effect of interfacial area on boron removal rate, of gas composition, mass of silicon and type of plasma on boron removal rate. Various results were achieved. The team showed that there is no change in deboronization rate during acceleration on bath agitation by high frequency induction heating, and that deboronization does not directly depend on plasma gas flow rate. Furthermore the team in every experiment reached less than 1 ppm presence of Boron. They claimed that boron removal rate is proportional to the steam and boron contents as well to the area of the dimple caused by the impinging gas jet, while is inversely

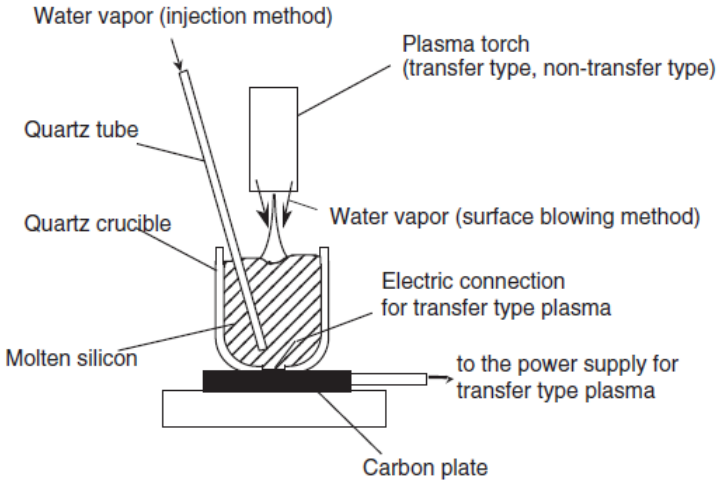

Figure 2.28: *Experimental setup [17]*

proportional to the mass of silicon. Boron removal rate actually increases when the hydrogen content of the impinging gas is increased. Non-transfer type plasmas were found to have a higher boron removal rate compared to transfer type plasmas under the same gas condition. A final result is that higher bath temperatures accelerate boron oxidation.

Chapter 3

Experimental

3.1 Overview

In this section, it will be described the experimental setup and the experiments performed in this thesis. In the next three Tables are listed the first set of ten experiments performed at NTNU laboratories. In addition to that, were considered in the analysis two more experiments that were carried out for another Master's Thesis under the same experimental conditions but at two different temperatures. Boron removal through gas refining was analysed with some fixed parameters: Temperature, Crucible type, Gas flow, Lance diameter. The crucible type chosen for all the experiments is the graphite. The parameters that were varied are relative to the mix composition of the refining gas, in order to better understand the role of the gases in the kinetics of the refining process. The variation of the other parameters were studied thoroughly by the NTNU group guided by J.Safarian et al.[19] and thus it was chosen to leave the them fixed. The quantity of Si, B and P were fixed for all the experiments, 400 grams of EG silicon doped with circa 40ppm of phosphorus and 10ppm of boron. Samples were taken at fixed timings for all the experiments.

In Table 3.1 are listed the first four experiments performed with pure hydrogen and humidified hydrogen at different percentages. In Table 3.2 are listed the experiments with Argon added to the mix at different percentages, while in Table 3.3 are the ones with Helium. In the last Table 3.4 are listed the extra experiments taken.

Table 3.1: List of first four experiments performed with parameters chosen.

Exp.	Gas Mix (vol%)	Gas Flow	Temp. [K]	Sampling[min]
1	H_2	5 [L/Min]	1823	0,10,25,45,75
2	$H_2 - 2\%H_2O$	5 [L/Min]	1823	0,10,25,45,75
3	$H_2 - 4\%H_2O$	5 [L/Min]	1823	0,10,25,45,75
4	$H_2 - 6\%H_2O$	5 [L/Min]	1823	0,10,25,45,75

Table 3.2: List of Experiments with Argon added to the blowing mix.

Exp.	Gas Mix (vol%)	Gas Flow	Temp. [K]	Sampling[min]
5	$50\%Ar - 50\%H_2$	5 [L/Min]	1823	0,10,25,45,75
6	$50\%Ar - 50\%H_2 - 4\%H_2O$	5 [L/Min]	1823	0,10,25,45,75
7	$75\%Ar - 25\%H_2 - 4\%H_2O$	5 [L/Min]	1823	0,10,25,45,75

Table 3.3: List of Experiments with Helium added to the blowing mix.

Exp.	Gas Mix (vol%)	Gas Flow	Temp. [K]	Sampling[min]
8	$50\%He - 50\%H_2$	5 [L/Min]	1823	0,10,25,45,75
9	$50\%He - 50\%H_2 - 4\%H_2O$	5 [L/Min]	1823	0,10,25,45,75
10	$75\%He - 25\%H_2 - 4\%H_2O$	5 [L/Min]	1823	0,10,25,45,75

Table 3.4: Extra experiments considered.

Exp.	Gas Mix (vol%)	Gas Flow	Temp. [K]	Sampling[min]
11	$H_2 - 4\%H_2O$	5 [L/Min]	1773	0,10,25,45,75
12	$H_2 - 4\%H_2O$	5 [L/Min]	1873	0,10,25,45,75

3.2 Experimental Procedure

3.2.1 Materials

Induction Furnace

The furnace utilized for the experiment is depicted in Figure 3.1 and has a maximum

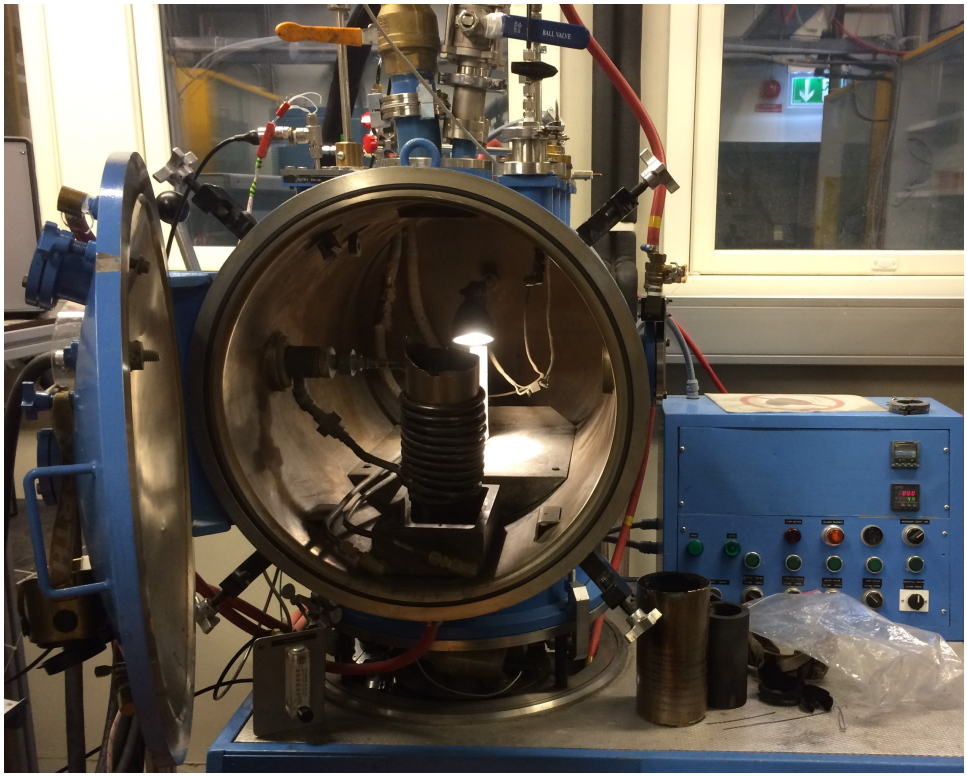

Figure 3.1: *Induction Furnace [courtesy of NTNU]*

power of 30 KW. For the experiments the power utilized varied from 3 to 6 KW, with a frequency of max 11.5kHz. It has a vacuum pump capable of reaching below $1.3 \times 10^{-3} mbar$ and a valve to control argon injection after vacuum conditions are created. It is important to understand why an induction furnace is the best technology to perform an experiment like that. First of all, induction heating is the process of heating a conductive object by means of electromagnetic induction [18], which is defined as the production of an electromotive force across a conductor through time varying

magnetic fields. As can be seen in the Figure 3.2 that represent the setup used in the project, it is noticeable a copper coil that surrounds a thermally non-conductive

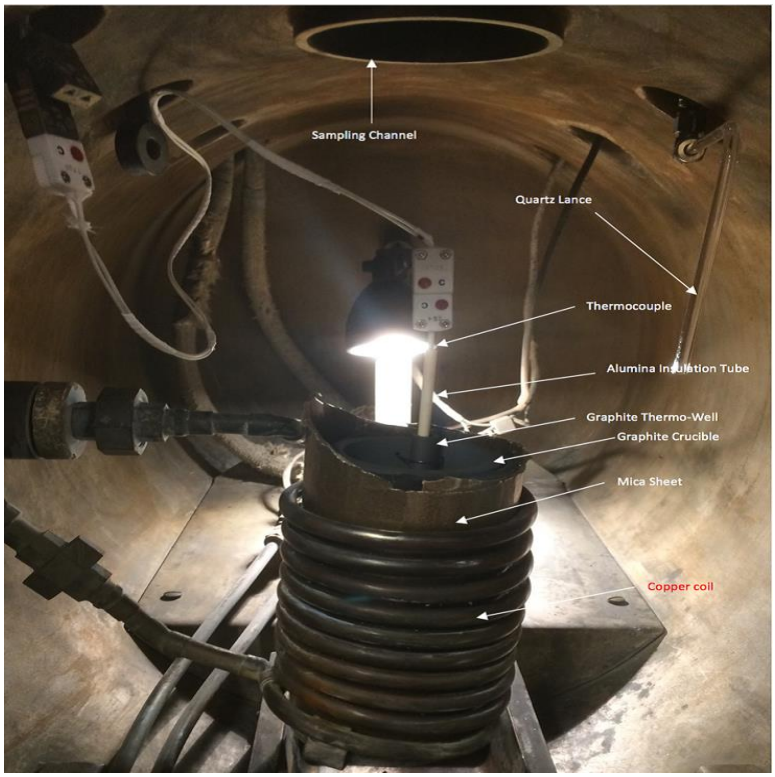

Figure 3.2: *Setup ready for the experiments [courtesy of NTNU]*

material, in this case, a carbon-wool inside a mica roll in which is disposed the refractory crucible that contains the melt that it is intended to be heated. A generator, produces a powerful alternating current that flows through the copper tube [18], the tube must be water-cooled in order to minimise copper heating.

The AC current creates a reverse magnetic field that penetrates the conductive crucible. By means of electromagnetic induction then *eddy parasitic currents* are created inside the graphite and through Joule effect, heat it up. It is important to underline that solid silicon is not conductive, thus it is heated through the graphite via radiation and conduction. A Scheme of the system is depicted in Figure 3.3 where 1 indicates the melt, 2 the water-cooled copper coil, 3 the yokes and 4 the crucible. It is important to

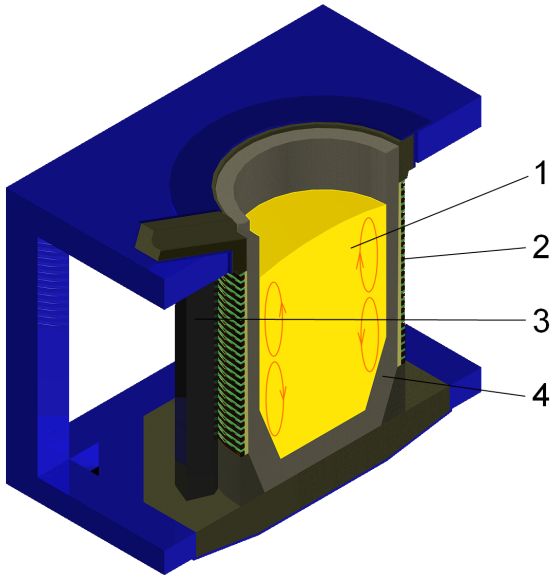

Figure 3.3: *Scheme of crucibe-coil system [courtesy of Christian Lindecke]*

observe that in the scheme is represented the process when Si already melt and thus became conductive.

As explained in [18] a big advantage of this kind of heating is that, once Si melted, the heat generated by means of eddy's currents cause vigorous stirring of the melt assuring a good mixing. Furthermore the heat is generated within the furnace's charge itself, avoiding contaminations and making possible to operate under vacuum conditions which would be otherwise not possible. The smaller the volume of the melt is, the higher the frequency that has to be used. This is due to the so-called skin depth, that is a measure of the distance an alternating current can penetrate beneath the surface of a conductor [18]. Utility frequencies go up to 400kHz, depending on material to be melted, capacity of the furnace and melting speed.

Crucible

The crucible chosen for the following experiments is a graphite cylindrical crucible, which has a good refractory quality having a much higher melting-point than silicon,

that melts at 1414 °C. Furthermore its high purity avoids contamination of the melt. A crucible for each experiment was needed. The dimension chosen were the following:

85mm Outer diameter, 70mm Internal diameter, 150mm Height

Other materials

For the experiments it was needed furthermore a graphite Thermo-well of dimensions :

200mm length, 14mm OD, 7-8mm ID

this needs to be placed in the crucible in order to allow the insertion of an alumina insulation tube of dimensions:

4mm ID, 6mm OD, 200mm length

which is needed to insulate the Thermocouple type-C used to measure the temperature of the melt. A crucial part of the experiment is of course the correct measure of the temperature in order to perform a good analysis. Color indicators [18] are common non-instrument measurements which involve the use of a temperature-sensitive painting in a pencil that is put in contact to the metal surface during the heating process but they are usually applied at a maximum temperature of 400 °C. In the temperature range of this experiment, the usual instrument utilized are the contact-type sensors(thermocouples) [18]. This instrument, via the *Seeback effect* produces a voltage proportional to the temperature of the junction of two dissimilar metals "A" and "B". This effect couples the thermal and electrical energies and allows temperature measurements with a simple analog or digital meter. The wires are electrically isolated except in the sensing tip, as can be seen in Figure 3.4

The Type-C definition, is related to the range of temperatures in which can be used and the materials, that in this case is a combination of Rhenium-Tungsten. The alumina

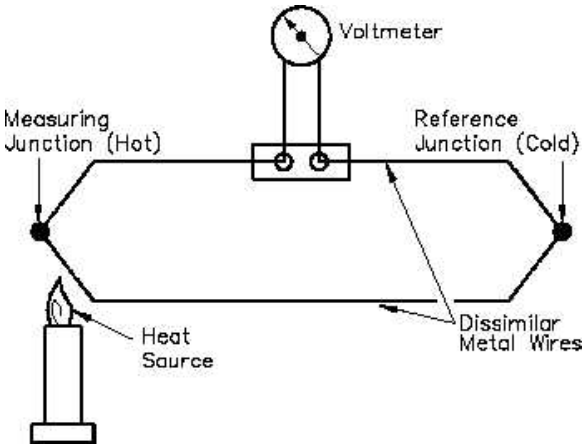

Figure 3.4: *Scheme of a thermocouple*

insulating tube is important to shield and protect the thermocouple from mechanical abuse and electromagnetic fields, that at high frequencies could alter measurements. Molybdenum wire was needed to ensure the connection between the thermo-well and the crucible after drilling two holes in the surface of the crucible. A thermocouple connector was needed, to communicate with the digital meter. Furthermore a mica roll and a carbon wool were used to thermally insulate the graphite crucible from the copper-coils. 20 quartz lances of 1 meter were ordered for sampling, and other quartz lances with a 90 degrees angle and a smaller internal diameter on the fixing side to make them more resistant, were needed to blow the gases on top of the crucible. Hydrogen, Argon and Helium were ordered to perform the experiments as well as two different flow meters, instruments crucial for the experiment since regulate the gas flow entering the furnace. A first one capable to handle solely the hydrogen flow, and another one of 10 [L/min] intended to handle the experiments with the mixtures of two gases. Finally, part of the experiments was also a moisturizer needed to humidify with a selected percentage the gases before entering the furnace.

3.2.2 Sample preparation and experimental setup

The experimental setup is shown in the Figures 3.1 and 3.2, and schematically is the same of Figure 2.18, with the exception of the different gases.

For every experiment, a graphite crucible is placed in the furnace, with a graphite thermo-well in which is inserted an alumina insulation tube with inside a type C thermocouple of $20cm$ length. The graphite thermo-well is locked to the crucible via a molybdenum wire. The crucible is placed in the water cooled copper coil inside a carbon wool and a mica roll, as seen in Figure 3.2, and locked with an insulating plate around the second ring of the coil.

Inside the crucible are placed 400g of solid silicon doped with 10ppm of B and 40ppm of P. The mixture of silicon was obtained mixing pure EG silicon with two silicon master alloys doped respectively with 500ppm of B and 1000ppm of P. To obtain the right proportion, 8 grams of Si-B (500ppm) and 4 grams of Si-P(1000ppm) were mixed with 388 grams of EG silicon.

The different gases are blown on top of the molten silicon through the $4mm$ diameter quartz lance which can be seen in Figure 3.2, which is placed $3.5cm$ above the molten silicon, circa in the center of the crucible. The temperature for all the experiments is kept at 1823K, except for the two extra ones at 1773K and 1873K. The exact distance of the quartz lance used for blowing was obtained calculating the volume that the 400gr of silicon would have occupied once melted with a simple calculation. The decided flow rate of gas was $5L/min$ and is controlled by the mass flow-meter connected to the gas tanks. Five samplings were performed for each experiment through a $1m$ quartz lance at different times: 0,10,25,45,75[min].

Its access to the furnace is possible through a port on top of it. The moisturizer uses distilled H_2O. There are windows in the furnace intended to be used to observe an eventual condensed phase on top of the molten silicon.

The resulting samples were carefully collected and sent to a laboratory in which they were studied through a ICP-MS (high-resolution inductively coupled plasma mass-spectrometer). This particular machine detects elements concentrations until one part in 10^{15}ppq. This is achieved through ionization of the sample with inductive coupled plasma to which is associated a mass-spectrometer that separates and identify the ions. In order to analyse the samples, they were crashed until pieces of approx. 2 mm of diameter and digested in a diluted mixture of 216 ml composed of $1,5HNO_3 + 0,5HCF$. Two parallels of each sample were taken, and the resulting concentrations of material were obtained averaging these two values. In some cases it was necessary to neglect the outliers.

3.3 Experiments Performed

A summary of the procedure followed will be now given for the various type of experiments performed.

3.3.1 Experiments with H_2 and $H_2 - (2, 4, 6)\%H_2O$ mixes

The procedure followed for the first four experiments was the following:
firstly the 400 grams of Silicon were prepared as described in the previous section, then the crucible, surrounded by the mica-roll and carbon wool was placed inside the copper coil. The blowing quartz lance was fixed to the machine and it was decided a length of 32cm for the sampling quartz, that was cut with a diamond knife. The sampling lance was connected to the sampling instrument. For the first experiment with pure hydrogen, the tube coming from the mass flow-meter, attached to the gas tank, was directly connected to the Furnace, to the blowing lance. The furnace was then closed and vacuum pump was activated. Vacuum is important in the process in order to remove

the air in the chamber, this is needed to create later the Argon atmosphere under which the experiments are taken. Once reached the desired pressure around $1.3 \times 10^{-3} mbar$ the argon valve was activated to break the vacuum. After that vacuum was made again. Argon was also injected in the sampling tube. At this point it was opened a valve to allow the flow of argon in and out of the chamber, in order to remove the volatile products created in the experiment. The Water circuit was opened in order to cool down the copper-coil during the experiment and hence the generator of the furnace was switched on. The power of the generator was varied slowly from 1 to 5 KW in order to reach and maintain the temperature of 1823K desired for the experiment. The first sample, namely "0", was taken once all the silicon melted and it was meant to be used to obtain the concentration reference of all the materials. After the the first sampling was performed, the blowing lance was moved above the melt and hydrogen flowing was started through the mass flow-meter, that was set to $5[L/min]$. The pressure selected from the tank was of 3 bar to have proper flow in the flowmeter, while the experiments were done at atmospheric pressure, circa 1 bar. From this moment, the stopwatch was activated and the next samples were taken at 10,25,45,75 [min].

For the three experiments with humidified hydrogen, the procedure followed was similar, with the difference that the tube coming from the mass flow-meter was connected to a moisturizer in order to humidify the gas. Thus, after the reference sample was taken, the moisturizer machine was activated and the blowing lance was put on top of the melt only when the selected percentage of humidification was reached.

3.3.2 Experiments with Ar/He in the mix

For these set of experiments the general procedure was the same of the previous experiments that used the moisturizer. The difference consisted in the fact that were needed two mass flow-meters, one that controlled the hydrogen flow and one that controlled

the Argon or Helium flow. In this way it was possible to select the percentage of the two gases in the total mix of $5L/min$.

3.3.3 Experiments with change in Temperature

The procedure for these two experiments was the same of the case of the humidified hydrogen. In both the experiments the percentage of humidification was set to be 4%, the only difference was the temperature at which the experiments were performed, 1773K and 1873K

3.3.4 Experimental challenges

During the experiments performed, numerous challenges were faced.
Handling hydrogen and avoid leaking was very important, a gas tube during the second experiment had to be substituted with the help of the supervisor, it was obstructed with silicon oxide and that avoided proper vacuum creation inside the chamber. The oscillation of the temperature of the melt was a major issue. It was extremely difficult to stabilise the temperature, it often tended to increase or decrease well above and under the level accepted. Timing was also a big challenge, it was very difficult to coordinate sampling and recording of time, temperature and pressure all together, two persons performing the experiment together were constantly needed. Finally it seemed very important to avoid the contamination of the samples collected. The procedure for a clean collection taught by the supervisor, was thoroughly followed to avoid the risk of incorrect sampling.

Chapter 4

Results and Discussion

4.1 Results

4.1.1 Experiments with $H_2 - \%H_2O$ mixtures at 1823K

In this section will be discussed the results coming from the first four experiments that have been carried out, relative to pure H_2 gas and H_2 gas humidified with 2,4 and 6 % H_2O. In Table 4.1 are reported the concentrations of Boron obtained in the five samplings. Each value, expressed in ppm, has been averaged out of the two parallel analysis performed in the laboratory and obtained out of the normalised value of Si in the melt. Outliers have been carefully excluded.

Table 4.1: Boron concentration for the first four experiments, expressed in ppm.

Time[min]	Pure H_2	$H_2 - 2\%H_2O$	$H_2 - 4\%H_2O$	$H_2 - 6\%H_2O$
0	8,47	10,58	10,90	8,40
10	8,33	/	8,85	8,03
25	7,58	7,57	5,49	/
45	7,17	5,46	5,19	5,08
75	7,05	3,18	2,66	2,72

In some of the experiments, samples at different timings were lost in the melt during

the procedure, but they didn't seem to affect the expected outcomes. These obtained values were used to analyse the trend of Boron removal. The concentration $C_B(t)$ over $C_B(0)$ and the mass transport coefficient $k_B = \frac{\ln(\frac{C_{B,0}}{C_{B,t}})}{(A/V)t}$ were the preferred instruments to describe the rate of Boron removal for all the cases. The ratio of Area over Volume was calculated for the crucible in use and it was found to be 24,5$[m^{-1}]$. The results of these calculations are summed up in the following Figures 4.1 and 4.2.

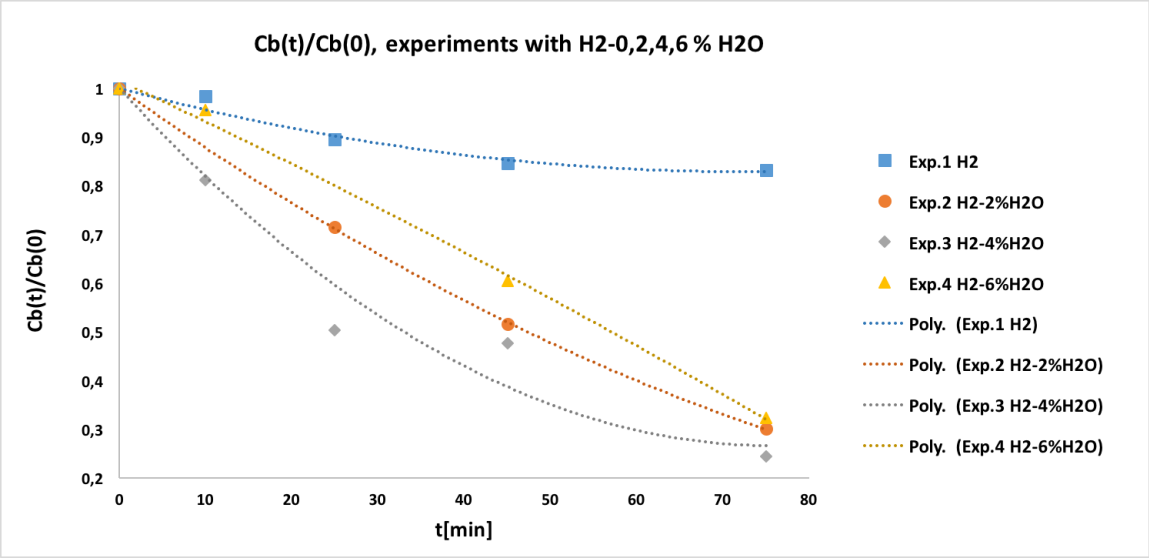

Figure 4.1: $C_B(t)/C_B(0)$ *trend for the first four experiments.*

In Figure 4.1 it is noticeable how while for H_2 and $H_2 - 4\%H_2O$ the trend is smooth and curvy, for the other two experiments the trend is different. This is merely caused by the absence of the samplings respectively at time 10 and 25 for these two cases that made polynomial interpolation more difficult. In Figure 4.2 is depicted a linear trend for $\ln(\frac{C_{B,0}}{C_{B,t}})$ over $(A/V)t$ which is in good agreement with the theory and previous literature [19] and confirms the first order assumption for Boron removal kinetics. Furthermore k_B values obtained from the interpolation are quite in accordance with the previous works [19].

It is quite apparent from both the figures and analysis how the best results in terms of

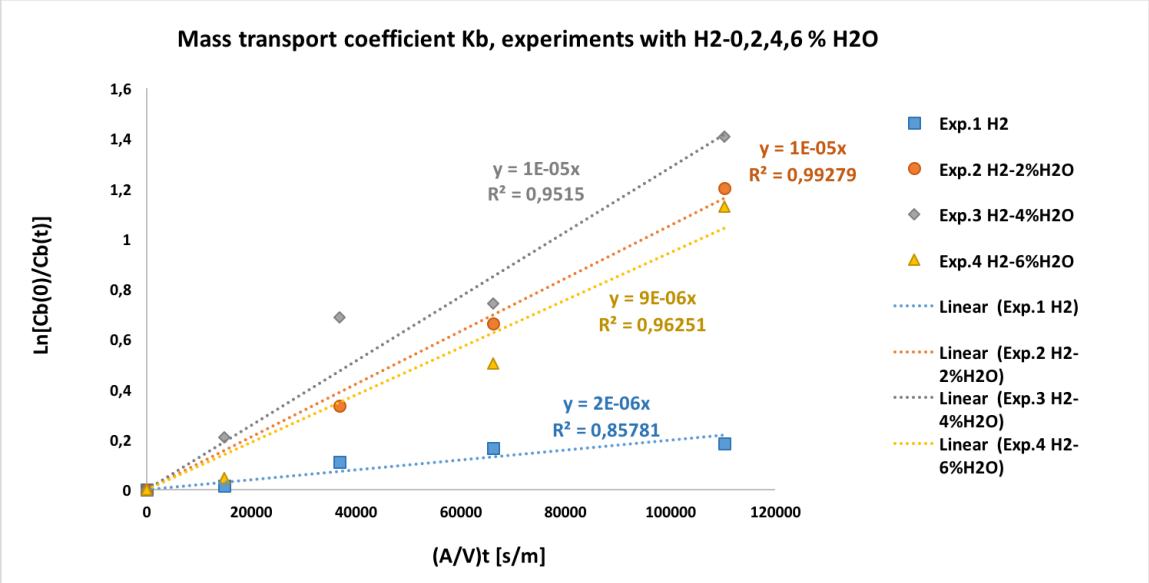

Figure 4.2: $\ln(\frac{C_{B,0}}{C_{B,t}})$ *over* $(A/V)t$ *trend for the first four experiments,* k_B *values are the x coefficients in the graph .*

Boron removal are obtained in the case of refining with $H_2 - 4\%H_2O$ while the worst result is obtained with pure H_2. This can be in the first place explained by the fact that with H_2 gas the biggest amount of volatile gases is in the form of B_xH_y products, while with humidified gases the presence of oxygen enhances HBO products. As already discussed, it has been proposed [19] that the dominant reaction driving Boron removal for humidified gases happens in the surface and it is described in the following form, $\underline{B} + \underline{H} + H_2O = HBO + \frac{1}{2}H_2$.

The hydrogen for HBO formation is provided by the $\underline{H}$ given by the blowing H_2 gas and by hydrogen present in the H_2O. The high solubility of H at the interface favours the reaction, but in order to obtain HBO species it is obviously crucial the presence of H_2O, that as already said, provides the oxygen for the formation of the volatile species. It also important to underline how the $H_2 - 2\%H_2O$ mix reveals itself to be more effective than $H_2 - 6\%H_2O$. This result is well in accordance with the previous literature [11], confirming the fact that the optimal humidification for H_2 is around 2-4%. Different

studies [5] [12] in fact, showed how boron removal rate increases with the oxygen or H_2O vapour concentration to the point that a layer of SiO_2 starts to form. When the layer is forming on the surfaces the boron removal rate tends to decrease significantly. This, in the various experiments, puts a limit on the concentration of oxygen that can be used, higher concentrations tend to block the reaction of oxidation of the boron, since oxidation of Si becomes a competitive reaction .

4.1.2 Condensate

During the experiments it was observed how for the humidified gases, inside the chamber there was a lot of evolution. Fumes started once the blowing lance was put inside the crucible, and were present throughout all the experiment. Once the chamber was opened, white condensate was found around the blowing lance and all inside the chamber. The results of the analysis, revealed a big amount of HBO species and SiO_2. This observation is in agreement with literature [19] and it can be explained considering that Si oxidates with the unreacted H_2O, that acts as oxidizing agent. It is interesting to report that during all the experiments no SiO_2 layer was observed, the reason for that is found in the high temperature utilised, in fact the NTNU team [12] showed that in their experiments above 1803K the SiO_2 layer wasn't observed at all.

They suggest, that the higher stability of $SiO(g)$ at higher temperatures reduces the possibility of layer formation. The NTNU team showed that the presence of H_2 suppresses the formation of the SiO_2 layer by oxidizing SiO in the gas layer, hence enhancing the diffusion rate of HBO products. For the experiment with pure H_2 on the contrary, almost no evolution was observed in the chamber during the experiment, and few traces of condensate were found. This confirms the important role of H_2O in the process of refining.

4.1.3 Experiments with $Ar/He-H_2-\%H_2O$ mixtures at 1823K

In this section will be analysed the set of six experiments regarding a combination of pure H_2 and $H_2 - H_2O$ mixtures with Argon and Helium gases. The concentration of boron in the various samplings is summarised in Table 4.2 and 4.3.

Table 4.2: Boron concentration for the Ar experiments, expressed in ppm.

Time[min]	$50\%Ar - 50\%H_2$	$50\%Ar - 50\%H_2 - 4\%H_2O$	$75\%Ar - 25\%H_2 - 4\%H_2O$
0	7,97	8,95	7,59
10	7,56	8,14	6,84
25	7,12	7,77	6,37
45	6,77	7,68	6,02
75	6,45	7,25	4,95

Table 4.3: Boron concentration for the He experiments, expressed in ppm.

Time[min]	$50\%He - 50\%H_2$	$50\%He - 50\%H_2 - 4\%H_2O$	$75\%He - 25\%H_2 - 4\%H_2O$
0	7,87	6,98	8,21
10	6,70	6,50	7,55
25	6,36	5,67	6,28
45	6,26	5,27	5,23
75	6,15	4,48	4,93

The results will be analysed separately and then summarised in a discussion in the next chapters.

Pure H_2 and $Ar/He - H_2$ Experiments Comparison.

In this subsection will be discussed the graphs representing $C_B(t)$ over $C_B(0)$ and $\ln(\frac{C_{B,0}}{C_{B,t}})$ over $(A/V)t$, relative to the experiments made with pure H_2, $50\%Ar - 50\%H_2$, $50\%He - 50\%H_2$ mixtures.

Trends are depicted in Figure 4.3 and Figure 4.4.

The two trends are quite clear and indicate how the experiment with pure H_2 is the one with the lowest rate of boron removal. Again we have a linear trend for $\ln(\frac{C_{B,0}}{C_{B,t}})$

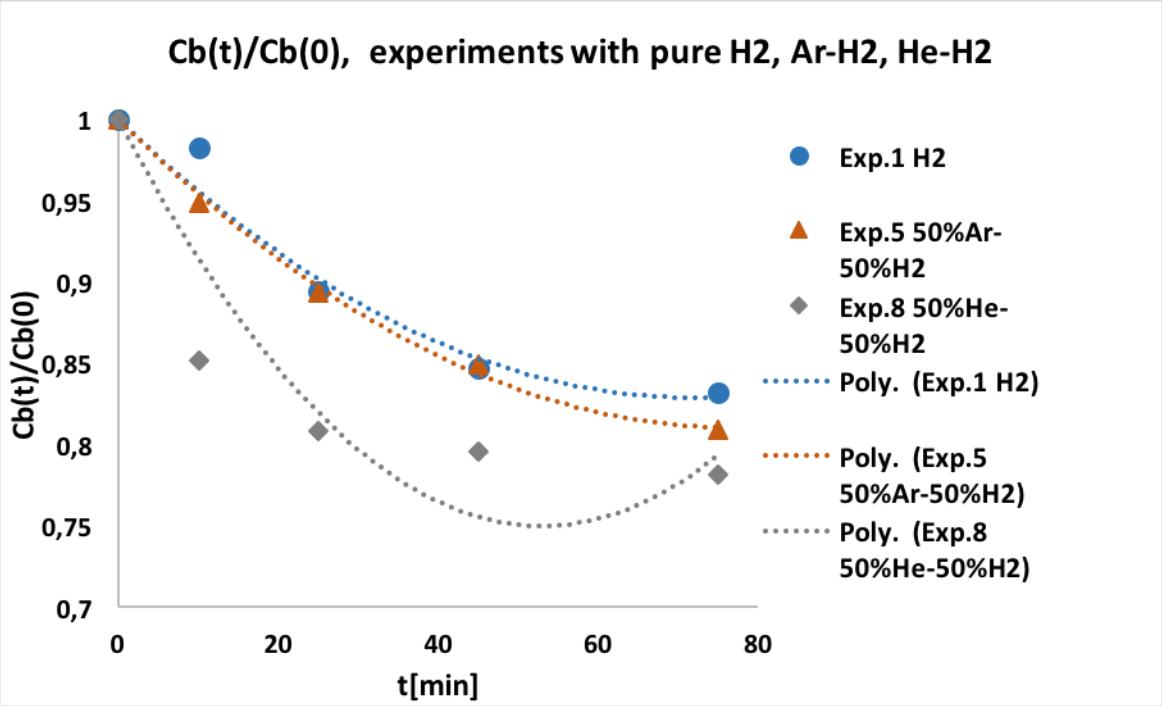

Figure 4.3: $C_B(t)/C_B(0)$ *trend for H2 and Ar/He-H2 mixtures.*

over $(A/V)t$ which is in good agreement with the theory and previous literature [19] and confirms also in this case the first order assumption for boron removal kinetics. It is interesting to notice that the experiments with Ar and He gases improve the performances with respect to the pure hydrogen experiment. This is due to a better kinetics of the process, in fact the two inert gases increase diffusivity and transport in the gas phase of the BH volatile products. It is a confirmation of what was found previously in literature [19] [13] hence, that mass transport in the gas phase is one of the most important factors that drives boron removal with gas blowing.

Another striking result is that the experiment with He lead to a better refining with respect to the experiment with Ar.

The reason behind the better results obtained by the experiments with Helium and the general improvement in diffusivity given by both the inert gases, has to be found in the *Maxwell-Stefan* equation diffusion model for multicomponent systems. In its simplest

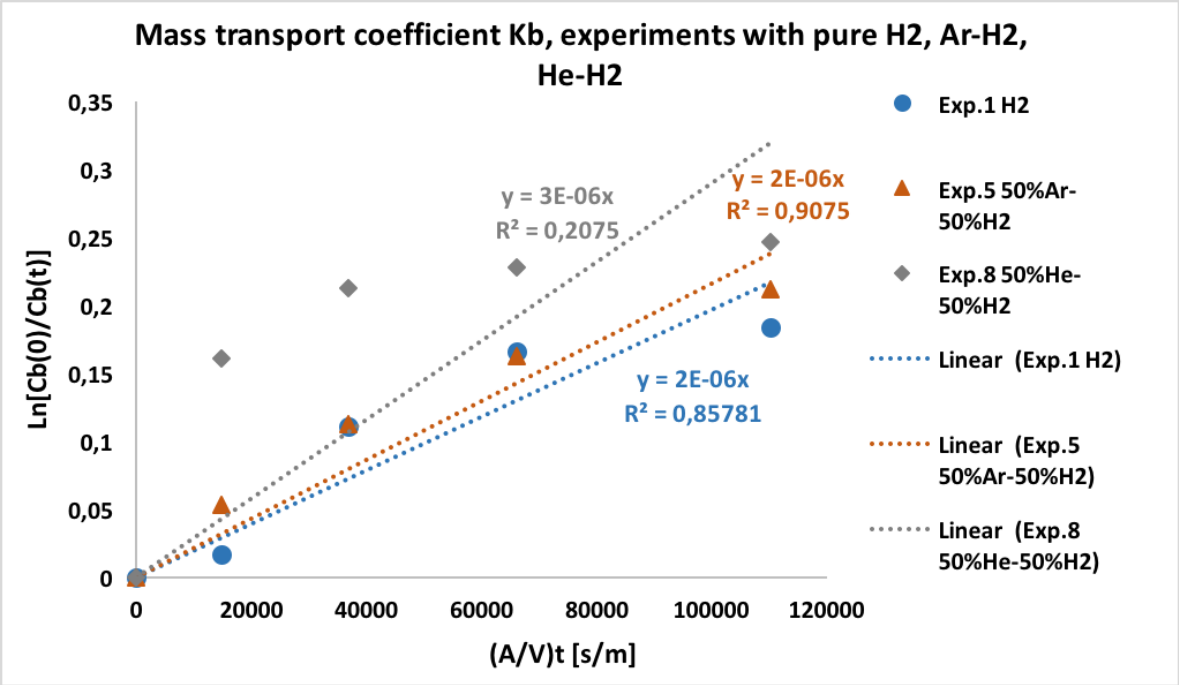

Figure 4.4: $\ln(\frac{C_{B,0}}{C_{B,t}})$ *over* $(A/V)t$ *trend for the Ar/He-H2 experiments,* k_B *values are the x coefficients in the graph.*

model, for a binary and ideal mixture of gas particles, has this form:

$$\nabla x_1 = -\frac{x_1 x_2 (\upsilon_1 - \upsilon_2)}{D_{12}} \tag{4.1}$$

where ∇x_1, is the diffusion driving force for species 1, x_2 represent the second species of gas particles, D_{12} is the binary diffusion coefficient that depends on temperature and pressure, and finally υ_1 and υ_2 are the diffusion velocities of the two gas species. The theory says that a diffusion flux is created when there is a deviation from equilibrium between molecular friction and thermodynamic interactions of the two species. In particular, the molecular friction difference is proportional to the difference in diffusion velocity of the species [20]. This means that if hydrogen is considered as x_1 and Argon or Helium as x_2, the difference in diffusion velocities of the two gases will contribute to create a diffusion flux. Hence, the addition of Argon or Helium in the mix, increases

the diffusivity of hydrogen. In conclusion, if it is considered the classical interpretation of the Maxwell-Boltzmann statistics for gases:

$$v = \sqrt{\frac{3kT}{m}} \tag{4.2}$$

where v is the velocity of the particle, m is the mass of the particle, T the temperature and k the Boltzmann constant, it is clear that a smaller particle mass leads to a higher velocity of the gas itself. With this in mind, it is easy to understand how Helium particles, that have a smaller mass with respect to the Argon ones and thus a higher velocity, create a difference between v_1 and v_2 that is higher compared to the one created by Argon, i.e., increasing the diffusivity of hydrogen. The better performance of He with respect to Ar is then related to its lightness.

Condensate for pure H_2 and $Ar/He - H_2$ Experiments

As for the H_2 experiment, the two experiments with He and Ar showed little evolution during the refining time, leaving the chamber with very few condensate on the lance at the end of the experiment.

$Ar - H_2 - \%H_2O$ Experiments Comparison

in this subsection will be analysed only the set of experiments performed with the use of Argon, 50% mixed with pure H_2, $50\%Ar - 50\%H_2 - 4\%H_2O$ and $75\%Ar - 25\%H_2 - 4\%H_2O$. Results are summarised in Figure 4.5 and Figure 4.6, in which are represented with the same methods of the previous sections.

The trends show how the rate of boron removal increases with humidification, as expected from the previous literature.

The Argon mixed with pure hydrogen has the poorest rate of boron removal among the three trends analysed. The best result comes when the Argon percentage in the mix is

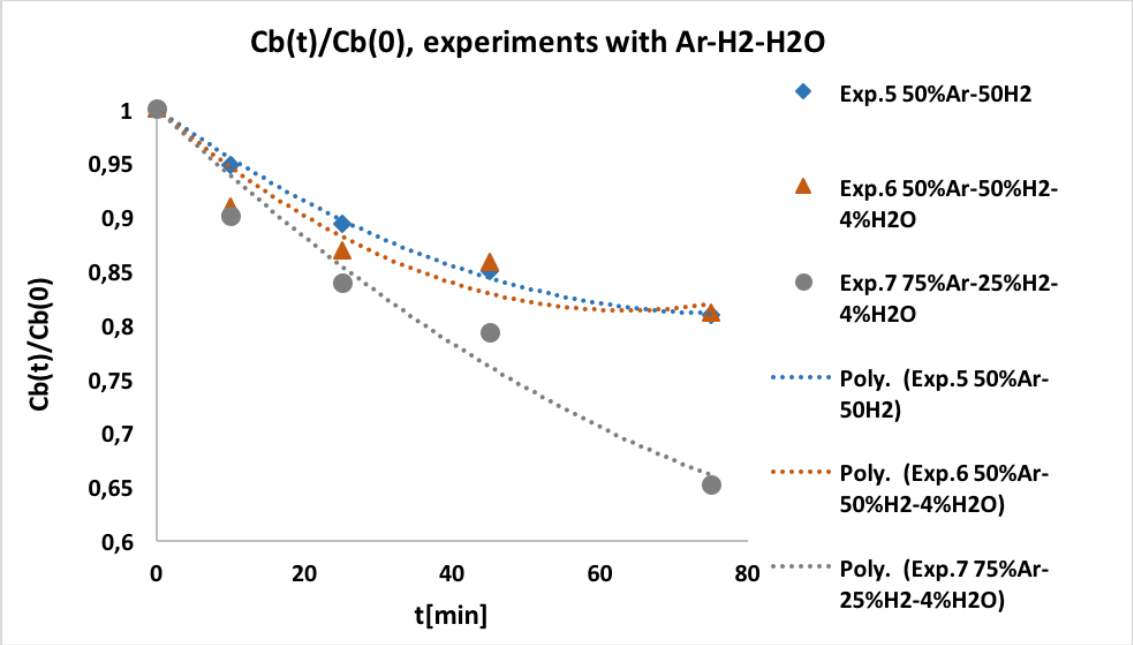

Figure 4.5: $C_B(t)/C_B(0)$ *trend for Ar-H2-H2O mixtures.*

75%. An explanation it was thought to propose for this, is that the higher ratio of $\frac{H_2O}{H_2}$ and thus the higher p_{H2O} in the case of $75\%Ar - 25\%H_2 - 4\%H_2O$, could increase the amount of $\underline{O}$ available for the reaction:

$$\underline{H} + \underline{B} + \underline{O} = HBO(g) \tag{4.3}$$

The increased $\underline{O}$ would then improve the creation of HBO(g) products. It can also be seen that the difference between the $50\%Ar - \%H_2$ and the $50\%Ar - 50\%H_2 - 4\%H_2O$ mixtures, is big for the first two samples while in the last two the points tends to be very close and the traced lines to overlap. This is in contrast with the trend of the graph of the same type that will be showed in the next subsection with He as the inert gas in the mixture. It was explained after watching the notes taken during the experimental session. In fact the quartz lance with the sample taken at minute 45 dropped in the melt, and another attempt of sampling immediately after had the same result. After the

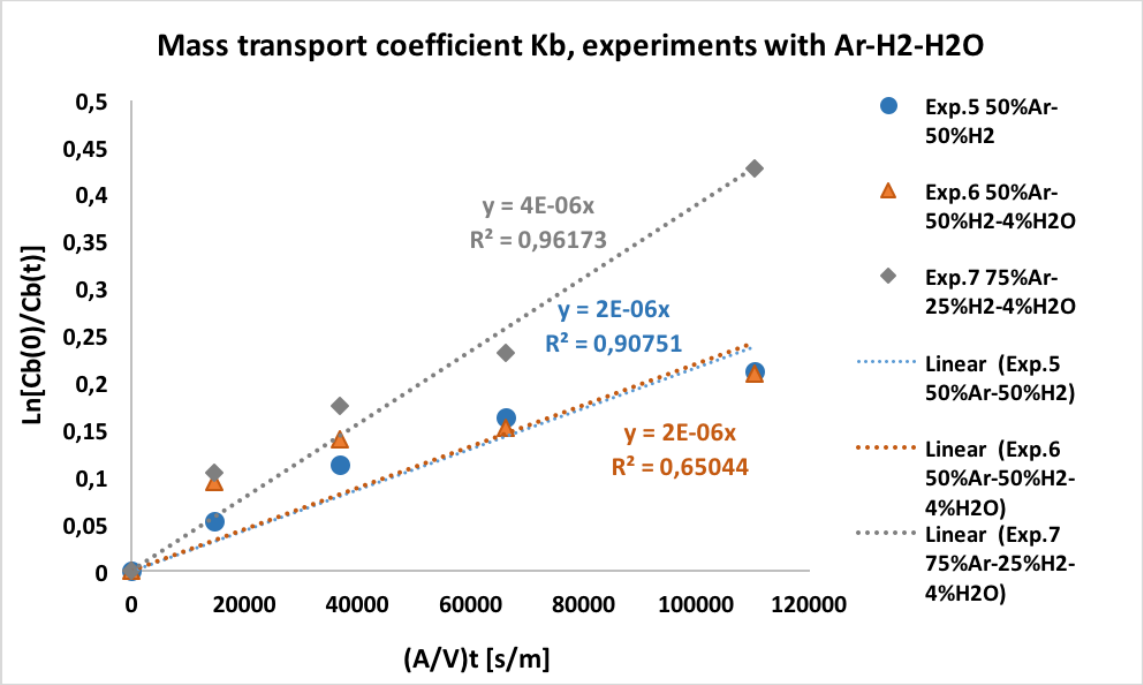

Figure 4.6: $\ln(\frac{C_{B,0}}{C_{B,t}})$ *over* $(A/V)t$ *trend for the Ar-H2-H2O experiments,* k_B *values are the x coefficients in the graph.*

experiment, the lances in the melt were extracted and the samples sent to laboratory, but the presence of the quartz lances must have influenced the process or boron refining since they acted as obstacles for the blowing lance and as impurities in the melt. If this accident didn't take place it would have been expected a trend symmetrical with the one of the He that will be showed later. This experiment is thus not entirely reliable.

$$K = \frac{a_{B2O3}^{1/2} \times a_{Si}^{3/4}}{a_B \times a_{SiO2}^{3/4}} \tag{4.4}$$

Condensate for $Ar - H_2 - \%H_2O$ Experiments

As expected, the experiment with less evolution and condensate deposition in the chamber was the the one with pure hydrogen in the mix, while the one with the most amount of fumes and condensate is the $50\%Ar - 50\%H_2 - 4\%H_2O$. This can be explained considering that the bigger amount of Argon in the 75% mix reduced the formation of

the condensate. It is also in accord with the observation that the biggest amount of condensate in the chamber was found in the first experiments, when $H_2 - H_2O$ mixtures were used. The amount of white deposition in the experiments in which Ar or He were added to the mix was observed to be clearly inferior to the previous ones.

$He - H_2 - \%H_2O$ Experiments Comparison

In Figure 4.7 and Figure 4.8 it can be observed the results for the experiments with $50\%He - 50\%H_2$, $50\%He - 50\%H_2 - 4\%H_2O$ and $75\%He - 25\%H_2 - 4\%H_2O$.

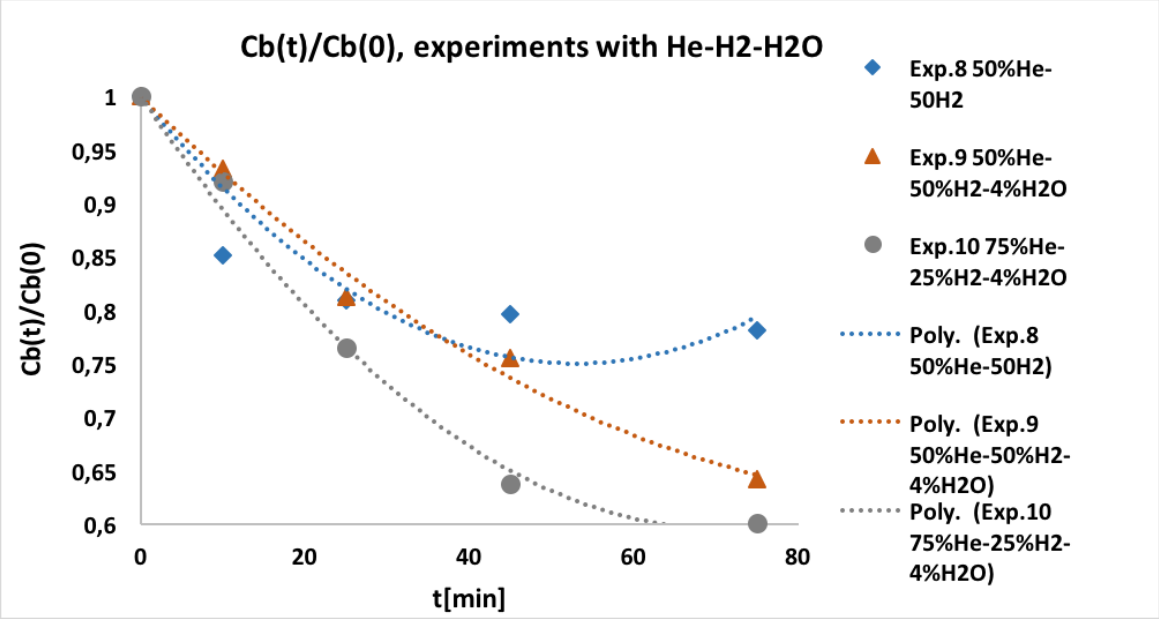

Figure 4.7: $C_B(t)/C_B(0)$ *trend for He-H2-H2O mixtures.*

Results confirms the same trend already saw for Ar, the best rate of boron removal is obtained when He in the mix is 75%, thus, were reached the same conclusions of the previous experiments.

It can be noticed how the two lines of $50\%He-50\%H_2$ and $50\%He-50\%H_2-4\%H_2O$ in this occasion do not overlap, this is due to a correct sampling during all the experiment that avoided to obstacle the process of refining, problem that was encountered during

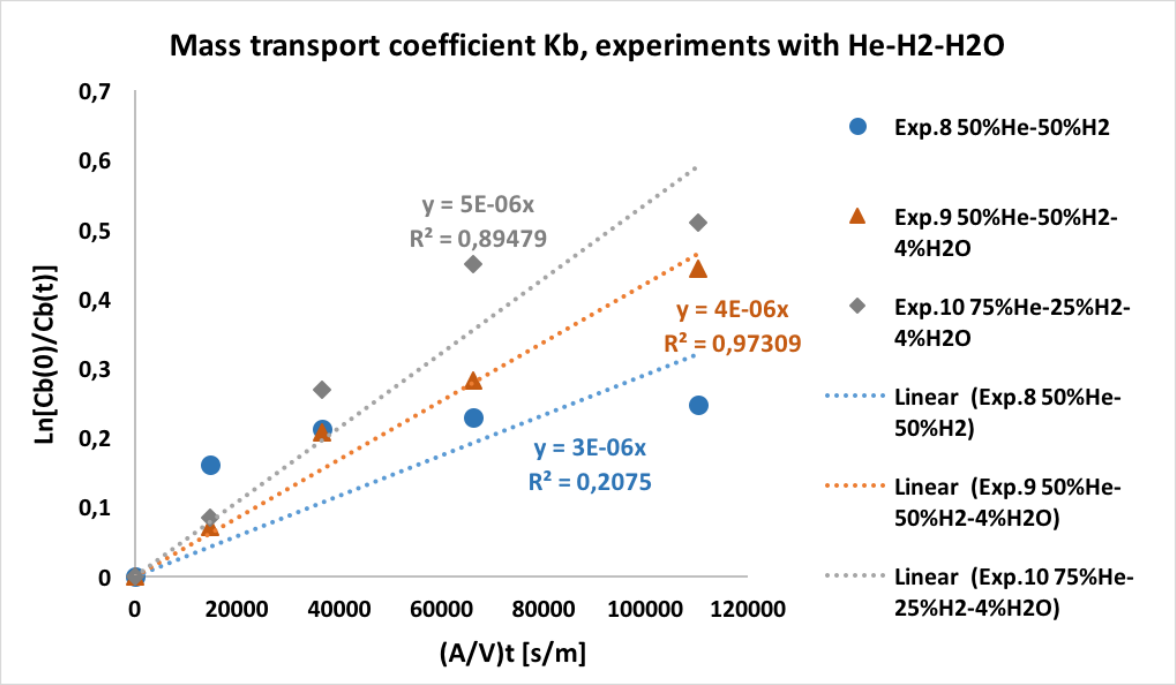

Figure 4.8: $\ln(\frac{C_{B,0}}{C_{B,t}})$ *over* $(A/V)t$ *trend for the He-H2-H2O experiments,* k_B *values are the x coefficients in the graph.*

the dual experiment with Argon.

Condensate for $He - H_2 - \%H_2O$ Experiments

The deposition observed in these experiments was lower than the previous ones, and the lowest was when 75%He was in the mix. The better diffusivity and mass transport of He compared to Ar, lead probably to a better dispersion of the condensate particles favouring their remotion by the Argon gas that flows in and out the chamber.

Comparison of $\ln(\frac{C_{B,0}}{C_{B,t}})$ over $(A/V)t$ for the six experiments with $Ar/He - H_2 - H_2O$ mixtures

From Figure 4.9 observation, it is confirmed what was expected. The humidified mixes gave better results compared to the pure H_2 mixes, since HBO formation is enhanced

and it adds up to the BH formation. Experiments with He as mixing gas, performed in general better than experiments with Ar gas, and mixes with 75%He or 75%Ar led to the best rates of Boron removal in the respective experiments. The reason proposed for that was already explained in the previous chapters. It is observed from the comparison of Figure 4.8 and Figure 4.6 that the linear trends differ instead of being symmetrical as expected because of Experiment 6, in fact its trend overlaps with the trend of Experiment 5. But this is due to the already discussed two samples that dropped in the the experiment with Argon. That would also explain why the Experiment 8 in Figure 4.9 has a higher trend than Experiment 6. In fact, since the presence of H_2O, Experiment 6 should have showed a better performance.

Comparison of Condensates of the six experiments with $Ar/He - H_2 - \%H_2O$

The lowest amount of condensate was observed in the He experiments, the reason for that was already explained.

In order to find a confirmation for the better refining performances found for both $75\%He-25\%H_2-4\%H_2O$ and $50\%He-25\%H_2-4\%H_2O$ with respect to the $75\%Ar-25\%H_2-4\%H_2O$ and $50\%Ar-50\%H_2-4\%H_2O$ mixes, it was analysed the condensate on the lance coming from two experiments, number 7, with $75\%Ar-25\%H_2-4\%H_2O$ gas mix and number 9, with $50\%He-50\%H_2-4\%H_2O$ mix.

It would have been better to have the condensates for the same percentage of the two inert gases, but unluckily not all the depositions of the experiments were collected. The output of the analysis anyway, doesn't change.

In Table 4.4 are represented, for the two experiments, the ratios of the concentration of B $[\mu g/g]$ in the condensate over the initial value of B $[\mu g/g]$ in the melt, sampled also at Time 0 [min]. The values were averaged over the two parallels used for the analysis of the samples. The goal of these calculations was to confirm the better refining obtained

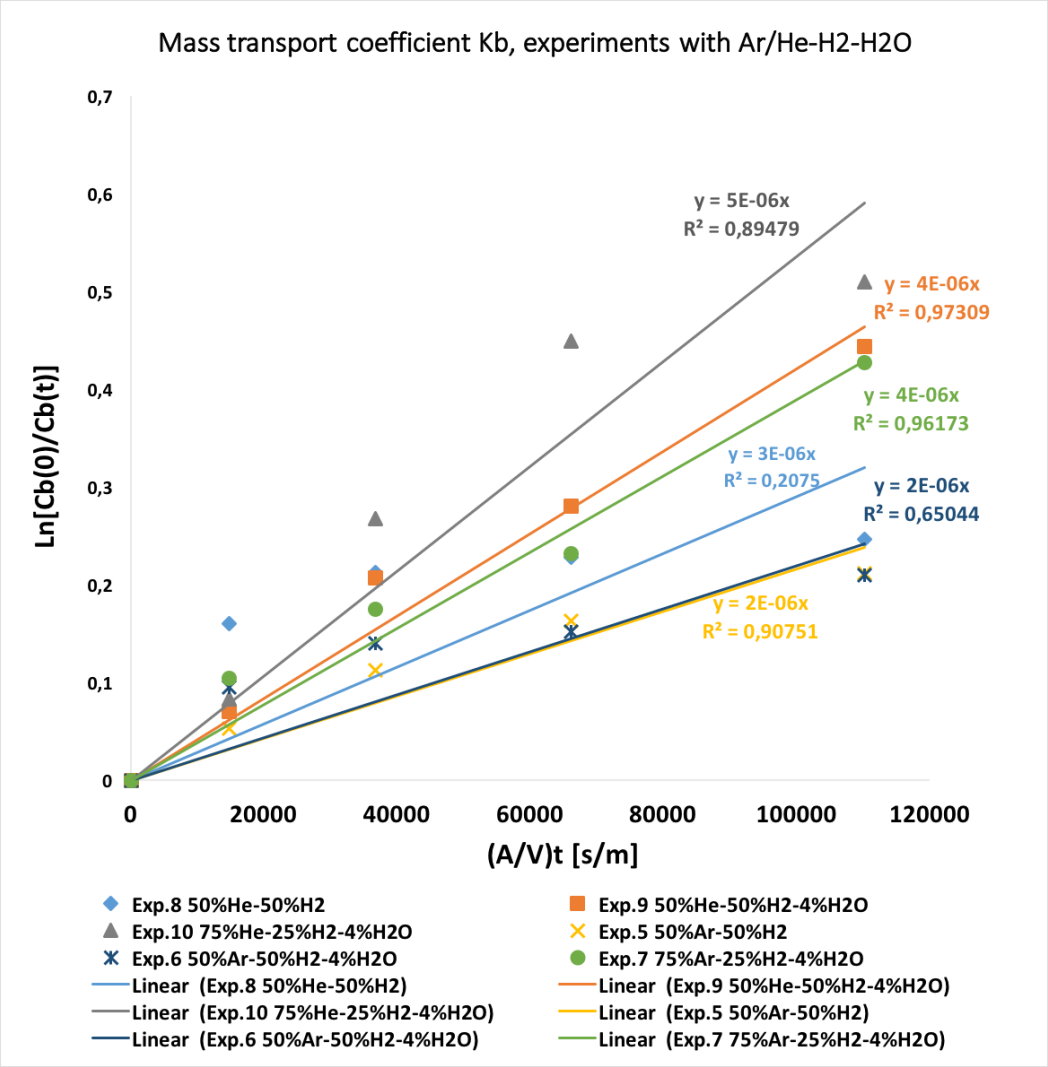

Figure 4.9: $\ln(\frac{C_{B,0}}{C_{B,t}})$ *over* $(A/V)t$ *trend for the six Ar/He-H2-H2O experiments,* k_B *values are the x coefficients in the graph.*

with the Helium in the mix.

Table 4.4: $C_B condensate/C_B(0)$ for Experiment 7 and 9.

Experiments	$C_B condensate/C_B(0)$
$7) 75\%Ar - 25\%H_2 - 4\%H_2O$	59,75
$9) 50\%He - 50\%H_2 - 4\%H_2O$	77,22

As can be seen clearly from 4.4 the amount of Boron present in the condensate of

Experiment 9 is higher compared to the one present in Experiment 7, this confirms the trends of better rate of Boron removal observed in the Experiment with He, depicted in Figure 4.9.

4.1.4 Phosphorus concentration

The concentrations of phosphorus throughout all the experiments were averaged out of the two parallels, but showed no sign of refining as can be observed in Figure 4.10 where all the values of the concentrations were plotted on time [min].

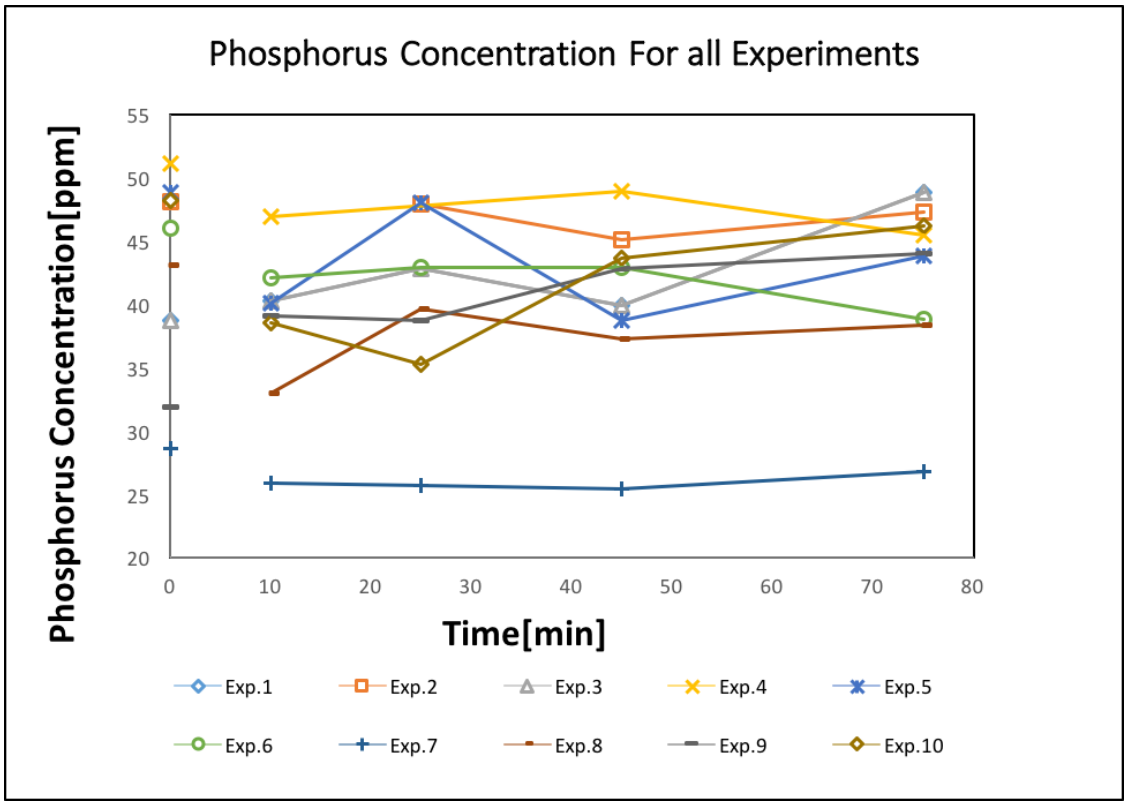

Figure 4.10: *Concentration of Phosphorus for all the ten experiments, measured in ppm.*

Refining by gas blowing alone is not effective for phosphorus removal, no remarkable volatile products seem to be created.

4.2 Discussion

4.2.1 Comparison of the ten experiments and discussion on results

In this section will be summarised the results on the ten experiments described in the previous discussions. To do so, it will be analysed Figure 4.11 in which is depicted the trend for $\ln(\frac{C_{B,0}}{C_{B,t}})$ over $(A/V)t$ for all the experiments performed.

Clearly the highest results in terms of rate of Boron removal were achieved by the experiments with pure H_2 humidified with $0, 2, 6\% H_2O$, with the best result with a percentage of humidification to be 4%. This is in accord with the previous literature [19], [13] that found for 2-4% of humidification the best results. This indicates that B removal through its direct reaction by H_2O is not favorable [19]. It was confirmed what has been stated in [19], e.g., that the experiments with an inert gas in the mix with hydrogen lead to a poorer rate of refining compared with pure humidified hydrogen.
It is interesting to notice in this optics how both Ar and He enhanced the boron refining when mixed only with H_2 thanks to their improvement to diffusivity and mass transport in the gas phase compared the pure H_2 mix, as showed already in Figure 4.4; while when the inert gases are added in big concentrations (50% and 75%) to the humidified gas, they actually reduce the efficiency of boron removal potential of the $H_2 - H_2O$ mix. This might be due to a reduction of Boron oxidation reactions caused by the inert gases, that reduce the area of contact between the species .
Hydrogen concentration importance was confirmed by other studies, Alteberend [5], in his Phd thesis, writes that boron removal rate increases up to 50% of hydrogen concentration, after this boundary overcomes saturation.
Suzuki et al.[5] attributed this effect to the thermal equilibrium between silica and $Si(l)$ at the surface, which shifts towards $Si(l)$ when hydrogen is added.

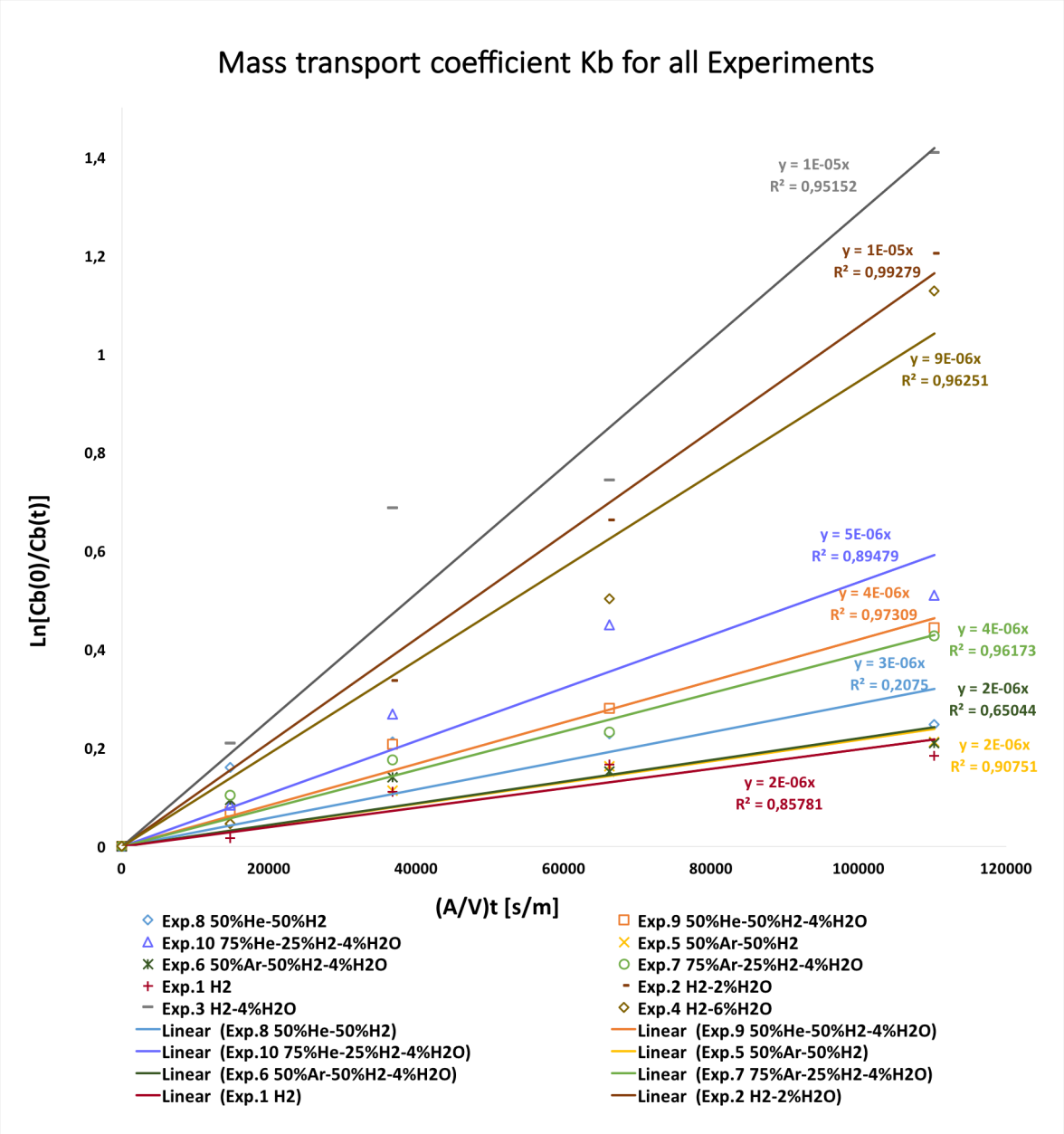

Figure 4.11: $\ln(\frac{C_{B,0}}{C_{B,t}})$ *over* $(A/V)t$ *trend for the ten experiments,* k_B *values are the x coefficients in the graph.*

4.2.2 Extra Analysis of $H_2 - 4\%H_2O$ mixtures at different temperatures.

It was found in the previous results that the best rate of Boron removal is obtained with $H_2 - 4\%H_2O$ mixes. The experiment was carried out at 1823K. It was thus decided to add the results of two more experiments that were carried out together with a series of others to gather information necessary for another master's thesis in the same field. The experiments were performed at +/- 50K and the concentration values of Boron are summarised in Table 4.5.

Table 4.5: Boron concentration for the two extra experiments, expressed in ppm.

Time[min]	$H_2 - 4\%H_2O$ at 1773K	$H_2 - 4\%H_2O$ at 1873K
0	8,76	7,73
10	6,14	7,01
25	5,93	/
45	4,24	3,66
75	3,59	2,38

The results in Table 4.5 were analysed with the same methods of the previous experiments and are depicted in Figure 4.12 and Figure 4.13.

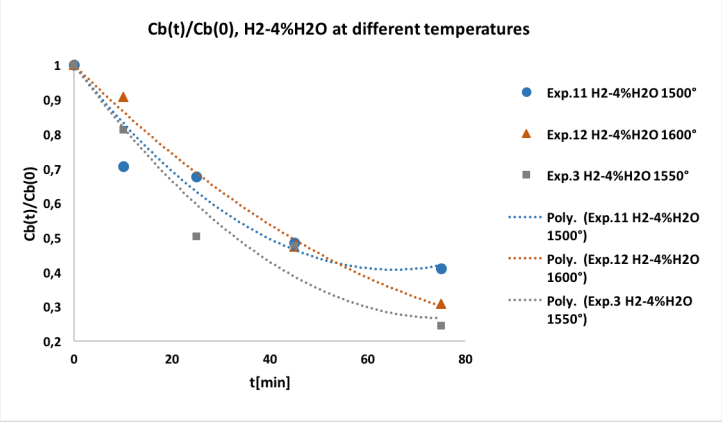

Figure 4.12: *$C_B(t)/C_B(0)$ trend for $H_2 - 4\%H_2O$ experiments at 1823K, 1873K, 1923K .*

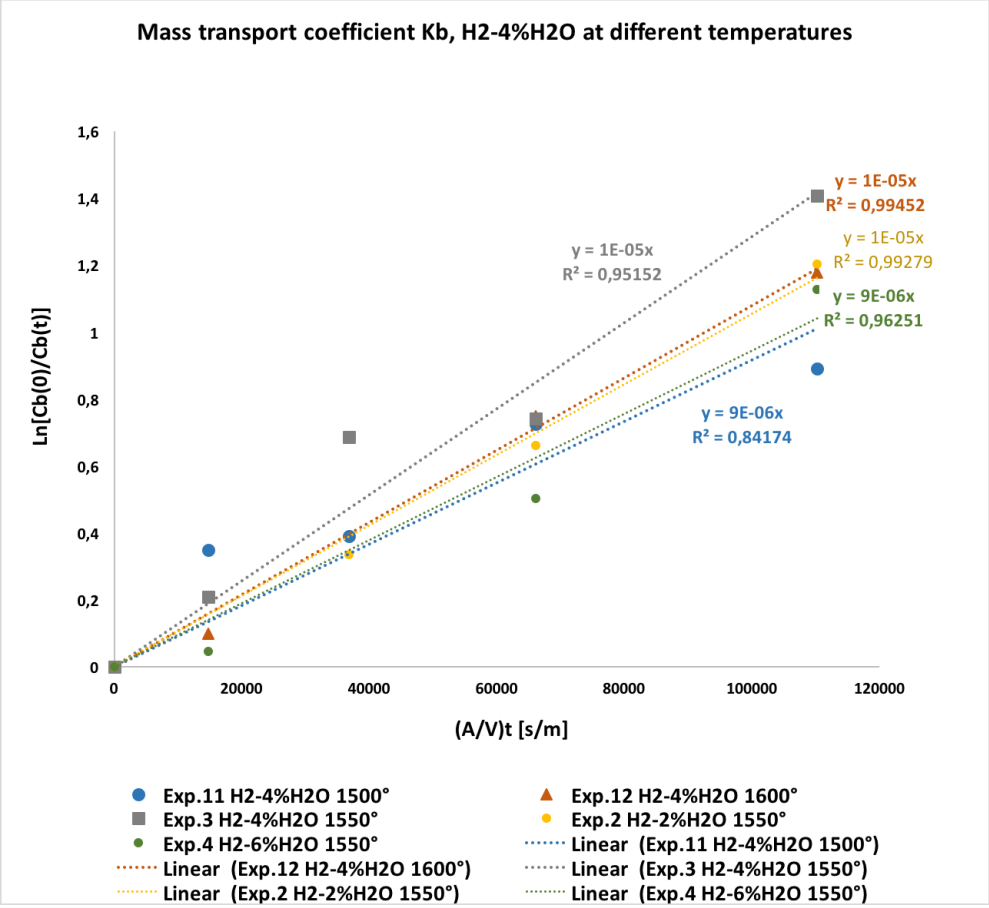

Figure 4.13: $\ln(\frac{C_{B,0}}{C_{B,t}})$ *over* $(A/V)t$ *trend for* $H_2 - 4\%H_2O$ *experiments at 1823K, 1873K, 1923K,* k_B *values are the x coefficients in the graph.*

The Trend of the graphs show how the temperature that leads to the best results for the $4\%H_2O$ is 1823K.

This is interesting since the results confirms the previous literature [12], [14] in which it is found that Boron rate removal decreases with the increasing of Temperature. In Figure 4.13 it was decided to plot also the k_B values for Experiment 2 and Experiment 4. It can be observed that Experiment 12 performed better in comparison to Experiment 2 and 4, while Experiment 11 in the comparison is the one with the lowest rate of Boron Removal.

4.2.3 Discussion on k_B parameters for the twelve experiments

In the next tables 4.6, 4.7 and 4.8 are summarised the k_B values found in the twelve experiments of this work and some of the ones found in experiments performed with graphite crucibles of the comparable size and similar experimental parameters, by the NTNU groups guided by J.Safarian et al.[19] and Nordstrand et al.[14]. The work carried out by J.Safarian et al.[19] concerned 400g EG-Si doped with 10-25ppm B. The refining process was fixed at 60 minutes and was carried out by a fixed gas mix of $H_2 - 3\%H_2O$ but different setup parameters, that will be summarized in Table 4.7. The experiments carried out by Nordstrand [14] in Table 4.8 concerned 200 EG-Si doped with 50-130ppm. Refining time in this case was 4.5 hours with sampling done every 30 minutes. Parameters like lance diameter and lance distance from the melt are not specified.

Table 4.6: k_B for the twelve experiments performed.

Experiments (vol%)	T[K]	Lance diameter [mm]	Lance distance from melt[mm]	Gas Flow[L/min]	k_B [m/s]
1)H_2	1823	4	35	5	2×10^{-6}
2)$H_2 - 2\%H_2O$	1823	4	35	5	1.1×10^{-5}
3)$H_2 - 4\%H_2O$	1823	4	35	5	1.8×10^{-5}
4)$H_2 - 6\%H_2O$	1823	4	35	5	9.4×10^{-6}
5)$50\%Ar - 50\%H_2$	1823	4	35	5	2.3×10^{-6}
6)$50\%Ar - 50\%H_2 - 4\%H_2O$	1823	4	35	5	2.4×10^{-6}
7) $75\%Ar - 25\%H_2 - 4\%H_2O$	1823	4	35	5	4.2×10^{-6}
8) $50\%He - 50\%H_2$	1823	4	35	5	3.2×10^{-6}
9)$50\%He - 50\%H_2 - 4\%H_2O$	1823	4	35	5	4.6×10^{-6}
10)$75\%He - 25\%H_2 - 4\%H_2O$	1823	4	35	5	5.6×10^{-6}
11)$H_2 - 4\%H_2O$	1773	4	35	5	9.1×10^{-6}
12)$H_2 - 4\%H_2O$	1873	4	35	5	1.3×10^{-5}

From the comparison between J.Safarian's paper [19] it can be observed that the k_B values that are obtained with the mix $H_2 - 3\%H_2O$ are in accord with the values in the present work with the similar mix $H_2 - 4\%H_2O$. For example, the experiment number 12, with flow rate $6[L/min]$, temperature of 1803K and lance diameter of $2mm$ gave a

Table 4.7: k_B for the experiments performed by the NTNU group [19] .

Experiments (vol%).	T[K]	Lance diameter[mm]	Lance distance from melt[mm]	Gas Flow[L/min]	k_B [m/s]
1)$H_2 - 3\%H_2O$	1703	4	30	0.5	2×10^{-6}
2)$H_2 - 3\%H_2O$	1703	4	30	1.5	3.3×10^{-6}
3)$H_2 - 3\%H_2O$	1703	4	30	3	1.3×10^{-5}
4)$H_2 - 3\%H_2O$	1703	2	30	0.5	1.5×10^{-6}
5)$H_2 - 3\%H_2O$	1703	2	30	1.5	5.1×10^{-6}
6)$H_2 - 3\%H_2O$	1703	2	30	3	9.4×10^{-6}
7)$H_2 - 3\%H_2O$	1703	2	30	6	1.9×10^{-5}
8) $H_2 - 3\%H_2O$	1703	2	30	9	2.5×10^{-5}
9)$H_2 - 3\%H_2O$	1703	2	10	6	1.3×10^{-5}
10)$H_2 - 3\%H_2O$	1703	2	50	6	1.7×10^{-5}
11)$H_2 - 3\%H_2O$	1803	4	30	3	7×10^{-6}
12)$H_2 - 3\%H_2O$	1803	2	30	6	1.3×10^{-5}

Table 4.8: k_B for the experiments performed by the NTNU group [14] .

Experiments (vol%).	T[K]	Lance diameter[mm]	Lance distance from melt[mm]	Gas Flow[L/min]	k_B [m/s]
5)$H_2 - 3\%H_2O$	1723	/	/	3	1.3×10^{-5}
6)$H_2 - 3\%H_2O$	1823	/	/	3	7.8×10^{-6}
7)$H_2 - 3\%H_2O$	1823	/	/	3	8.7×10^{-6}
8)$H_2 - 3\%H_2O$	1873	/	/	3	7.9×10^{-6}
11) $75\%Ar - 25\%H_2 - 3\%H_2O$	1773	/	/	3	4.3×10^{-6}
12) $50\%Ar - 50\%H_2 - 3\%H_2O$	1773	/	/	3	8.4×10^{-6}
13) $25\%Ar - 75\%H_2 - 3\%H_2O$	1773	/	/	3	9.2×10^{-6}

value of k_B very similar to the experiment performed in this work with $H_2 - 4\%H_2O$ at 1823K. The small negligible difference could be explained by the higher amount of H_2O present in the experiment performed for this thesis, that balances the difference between diameter of the blowing lances. The differences in the other experiments are well explained in the paper [19] that indicates how a higher flow-rate of hydrogen, a smaller lance diameter and a temperature close to the melting point of the silicon give the best results in terms of rate of Boron refining. In fact the highest value of k_B in the paper is reached in Experiment 8.

A comparison between the values of k_B coming from Nordstrand's paper [14] for the

experiments with $H_2-3\%H_2O$ at 1823K and 3[L/min] with the experiment performed in this work with a mix of $H_2-4\%H_2O$, in absence of the other parameters, confirm that at the same temperature of 1823K, the higher flow-rate of 5[L/min] gives a slightly better refining rate of Boron. The results coming from the mix with Argon in experiment 11 and 12 of the same paper instead give a different picture than the one obtained in this work for Argon and Helium. In Nordstrand's work the best refining rate was obtained with the $50\%Ar-50\%H_2-3\%H_2O$ mix, the opposite of what was found in this Thesis. Furthermore much higher k_B values were found in their work with the same percentage of argon in the mix. A comparison of the results obtained in this research with the ones of Nordstrand is depicted in Figure 4.14.

It can be clearly seen how the trends differ for the experiments. It has to be said that the differences between the quantities of silicon, the quantity of boron, Flow-rate, temperature and refining time (4.5 hours) might influence the output of the process leading to different results. In any case, more experiments on this mixtures of gases with similar experimental conditions have to be carried out to understand better these differences.

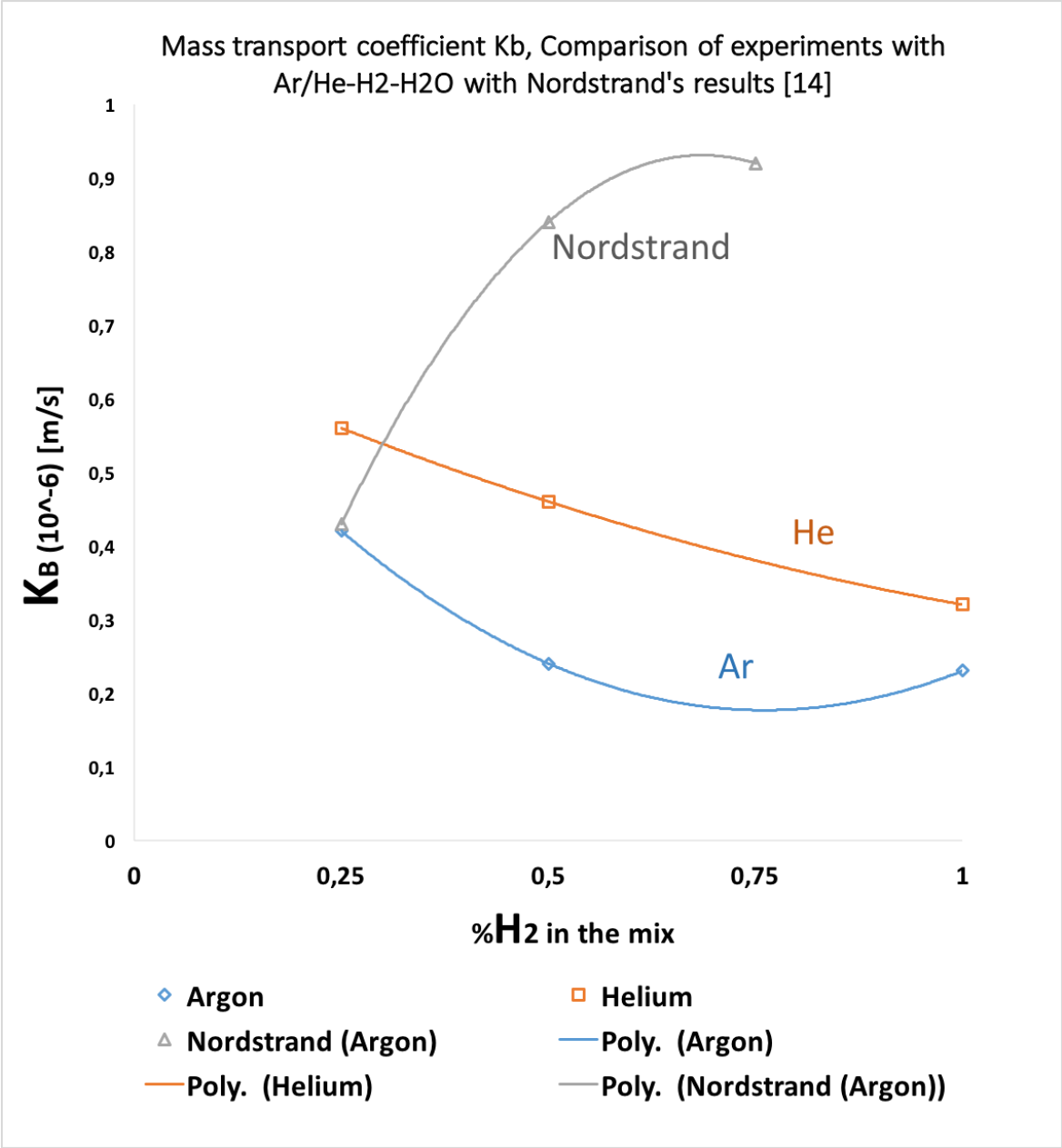

Figure 4.14: *k_B comparison for the experiments with Argon and Helium (no. 5 to 10) of this thesis and experiments no. 11,12,13 of Nordstrand's paper [14].*

Chapter 5

Conclusion

5.1 Conclusion

Boron removal via gas blowing using different mixes of $Ar/He - H_2 - H_2O$ gases was the subject of this Master Thesis. 10 experiments at a fixed temperature of 1823K plus 2 at temperatures of 1773K and 1873K were performed in the NTNU laboratories.
The main conclusions are listed below.

• The experiment with $H_2 - 4\%H_2O$ mix of gases, was the best of all experiments in terms of Boron removal and its k_B value is in accord with the previous literature, [19].

• The comparison between He and Ar showed that He, given its lightness, has a better diffusivity and and mass transport in the gas phase.

• Another interesting result was that in both experiments in which Argon and Helium were used in the blowing mix with pure Hydrogen, the Boron removal was enhanced, this can be explained considering the increase of diffusivity that is brought by the two inert gases that leads to a better transport of BH products away from the surface.

• Phosphorous impurities in the melt were not removed, this technique had no effect on phosphorus concentration in every experiment.

• It was found that experiments with 75%-25% ratio mixes of both Argon and Helium with humidified hydrogen showed an improved Boron removal compared to the 50%-50% ratio, which is in disaccord with the trend found in the paper [14]. A mechanism that explains the reason for a better removal of the 75%-25% ratios for both the gases was proposed, but it must be confirmed with more experiments on these mixes of gas.

Chapter 6

Outlook

6.1 Outlook

The results obtained in this work are just indicative and not conclusive, and the Hypothesis proposed must be analysed more thoroughly with more experimental analysis of mixture of gases. Nevertheless it was demonstrated and confirmed that the gas blowing technique is a valid way to remove Boron from melt silicon, more research should be carried in the future on different mixtures of gases in order to find the best combination for Boron removal and to better understand the chemistry and kinetics of Boron removal, that yet has not be comprehended fully.

Chapter 7

Appendix

7.1 Appendix

In this appendix are listed the trends of the variation of concentration of Boron in the experiments.

7.1.1 $C_B(t)$ in the various experiments

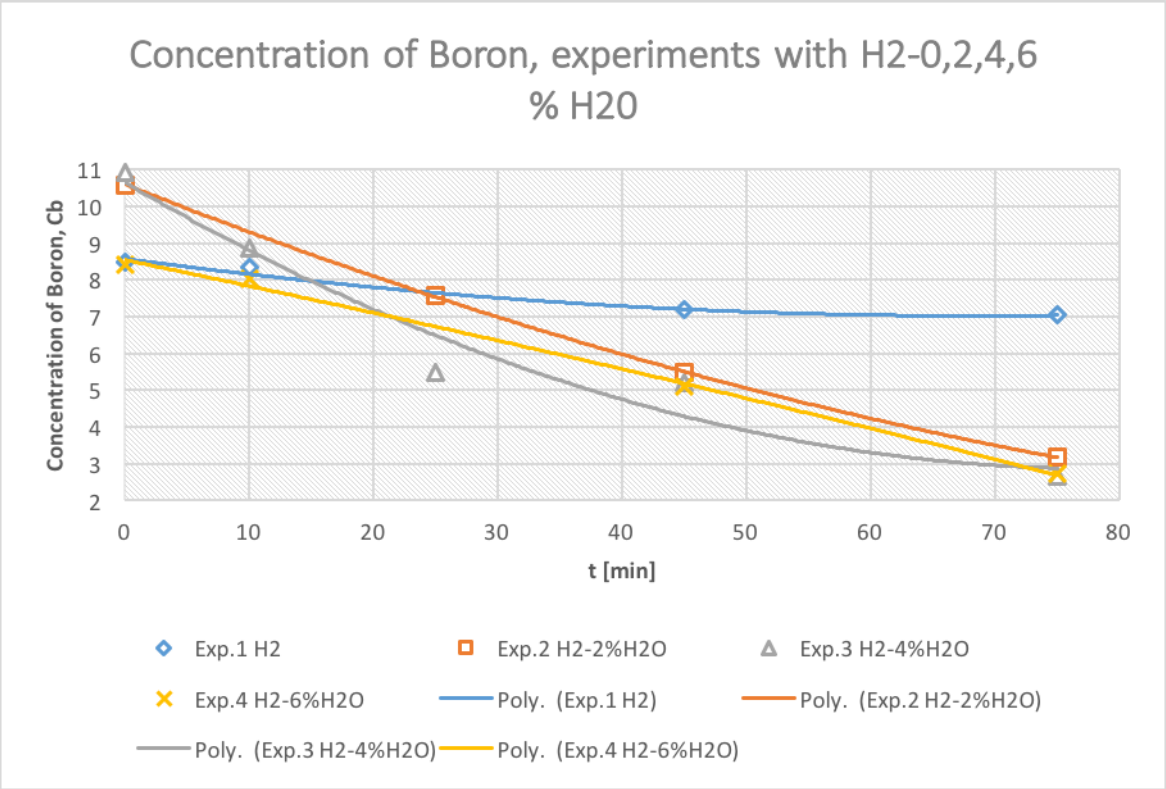

Figure 7.1: $C_B(t)$ *trend.*

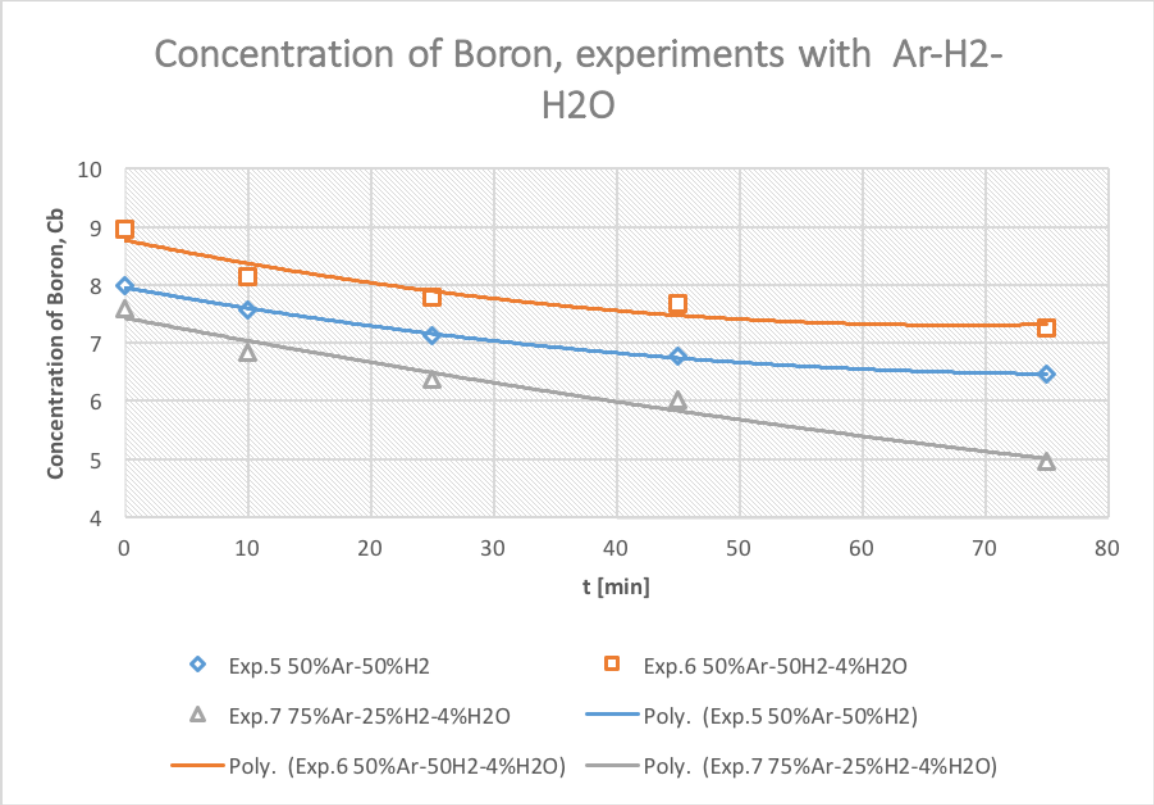

Figure 7.2: $C_B(t)$ *trend.*

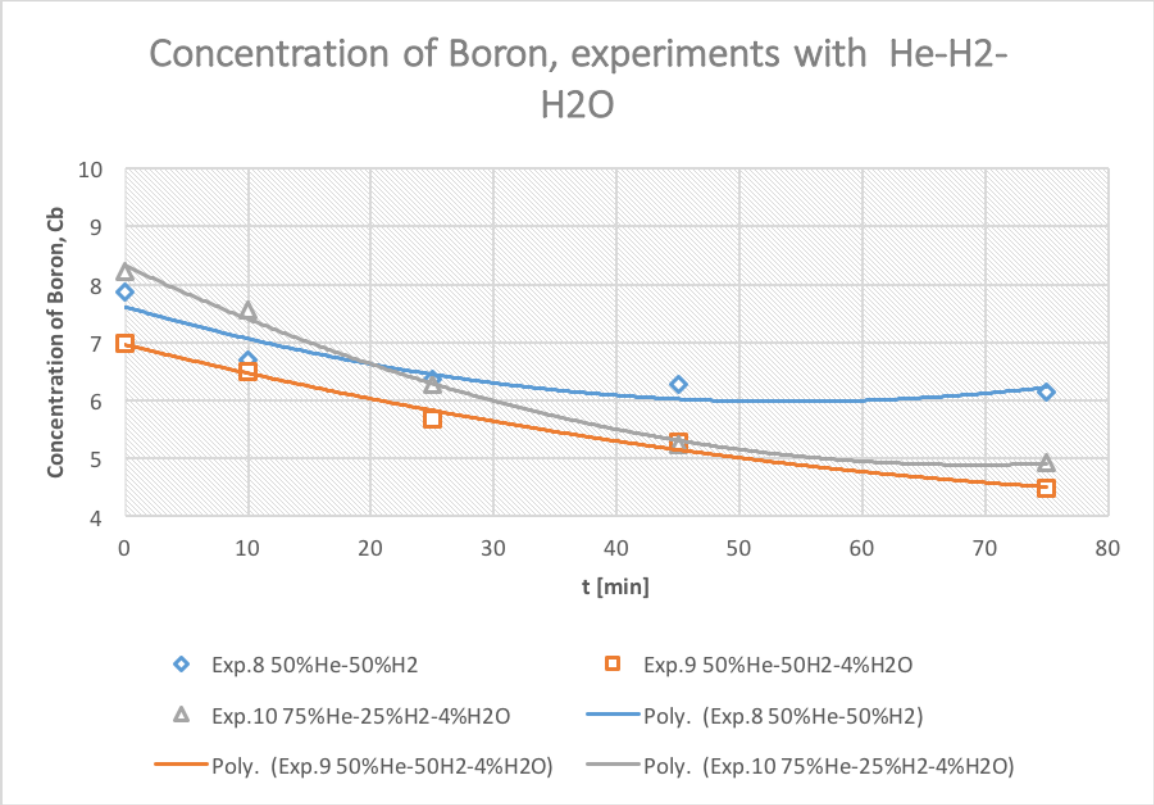

Figure 7.3: $C_B(t)$ *trend.*

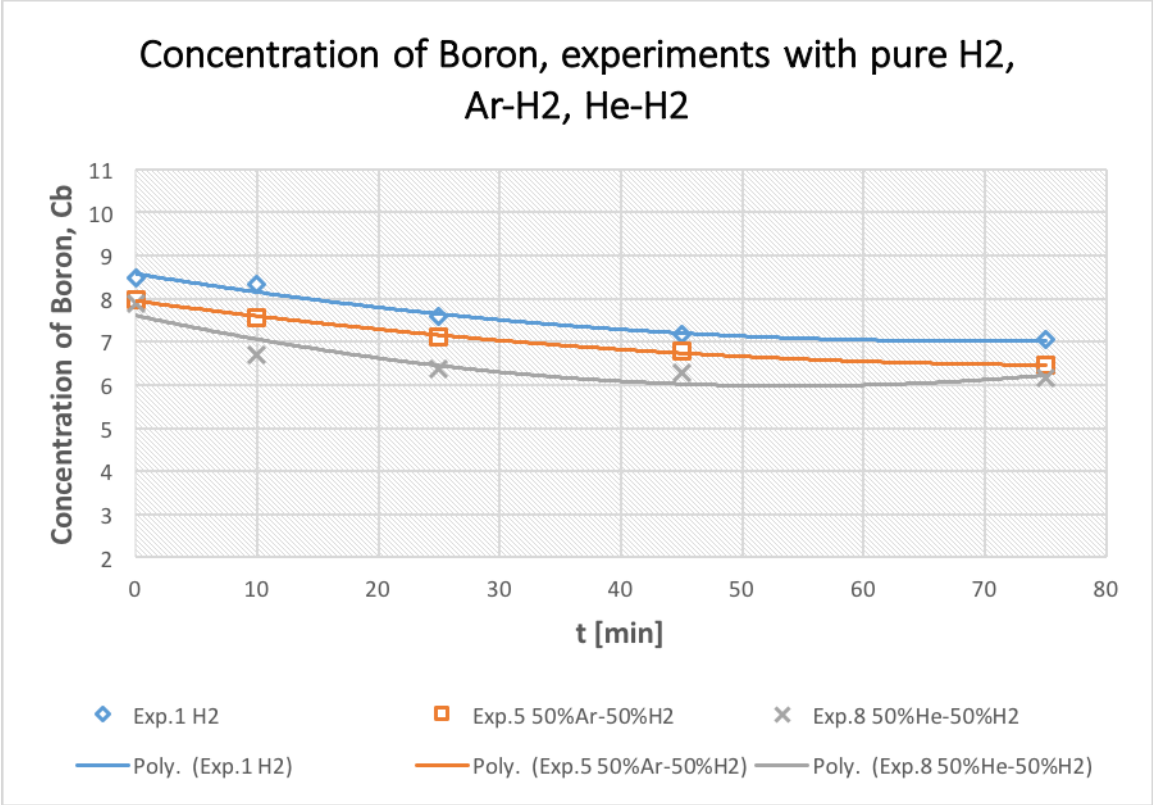

Figure 7.4: $C_B(t)$ *trend.*

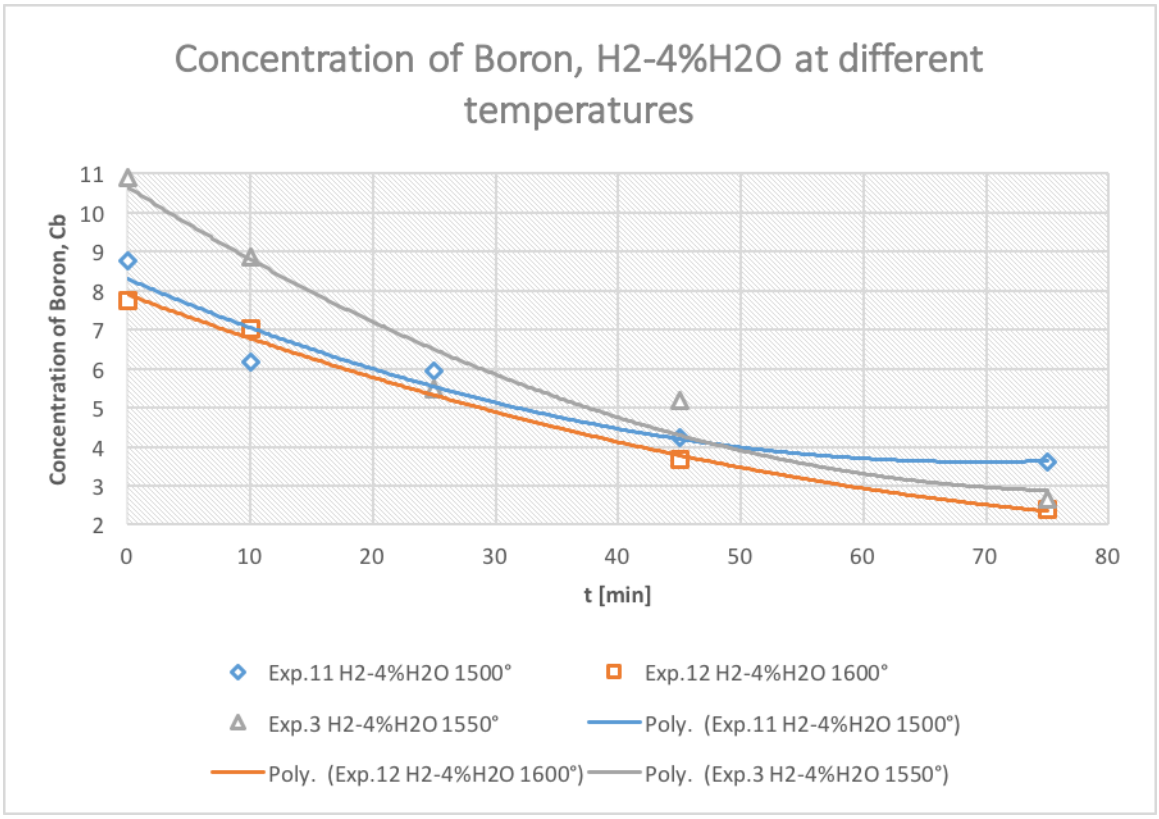

Figure 7.5: $C_B(t)$ *trend.*

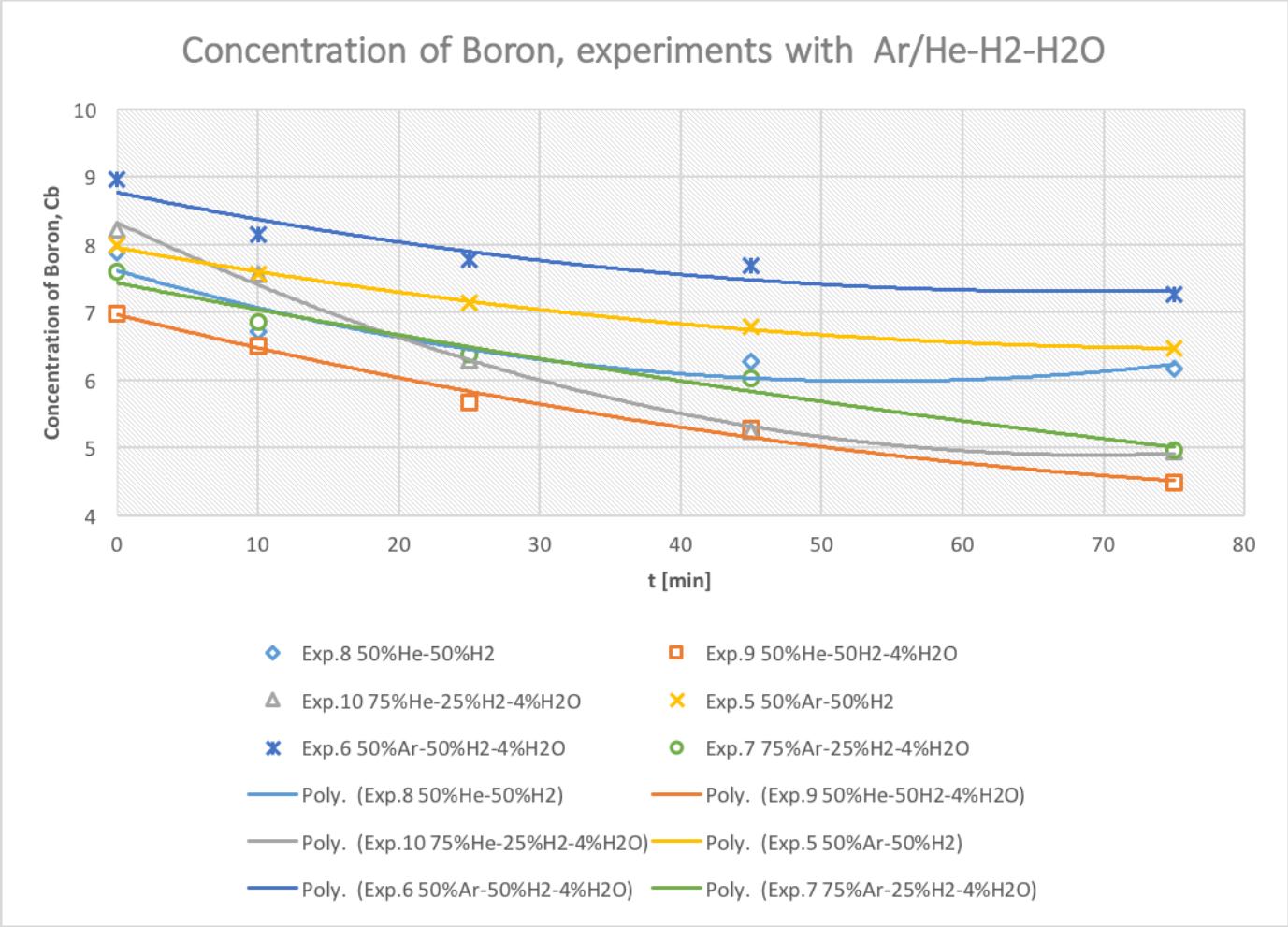

Figure 7.6: $C_B(t)$ *trend.*

Bibliography

[1] Morita, Yang Bin et al., *Boron removal from metallurgical grade silicon by oxidizing refining, 2008*

[2] Khattak et al., *A simple Process to remove boron from metallurgical grade silicon 2002*

[3] Yasuda et al., *Production of Solar-grade silicon by Halidothermic reduction of silicon tetrachloride, Metallurgical and Material transactions B 42:37*

[4] Flamanta et al., *Purification of metallurgical grade silicon by a solar process,Solar energy materials & solar cells, 2006, 90(14): 2099-2106*

[5] Jochen Altenberend, *Kinetics of the plasma refining process of silicon for solar cells: experimental study with spectroscopy, Grenoble university, 2012*

[6] H.C Theurer, *Trans.Am.Inst.Min.Metall.Eng, 1956, vol 206 (10)*

[7] Dietl and Wohlschlaeger, *Process for purifying metallurgical-grade silicon, 1981*

[8] Larss Klemet Lakobsson, *PhD thesis, 2013*

[9] Gabriella Tranell, *TMT 4236 course materials NTNU, 2015*

[10] Krystad, G.Tranell, *The kinetics of boron transfer in slag refining of Silicon, 2012*

[11] Nordstrandet al., *Removal of Boron in Silicon by H2-H2O gas Mixtures, 2012*

[12] J.Safarian, G.Tranell, *Boron removal from silicon by humidified gases, MMTE 2014*

[13] Sortland, Tangstad, *Boron removal from silicon melts by H2O/H2 Gas blowing: mass transfer in gas and melt, 2014*

[14] Norstrand et al., *Removal of boron from silicon by moist hydrogen gas, Springer, N.p , n.d. Web 14 Nov 2015*

[15] Fourmand et al., *Refining of metallurgical silicon for crystalline solar cells, 2004*

[16] Alemany et al., *Refining of metallurgical-grade silicon by inductive plasma, 2002*

[17] Nakamura et al., *Boron Removal in molten silicon by a steam-added plasma melting method, 2004*

[18] Rudnev et al., *Handbook of induction heating, 2003*

[19] J.Safarian et al., *Mechanisms of kinetics of Boron removal from Silicon by humidified hydrogen, 2015*

[20] S. Rehfeldt, J. Stichlmair, *Measurement and calculation of multicomponent diffusion coefficients in liquids, Fluid Phase Equilibria, 2007, 256, 99-104*